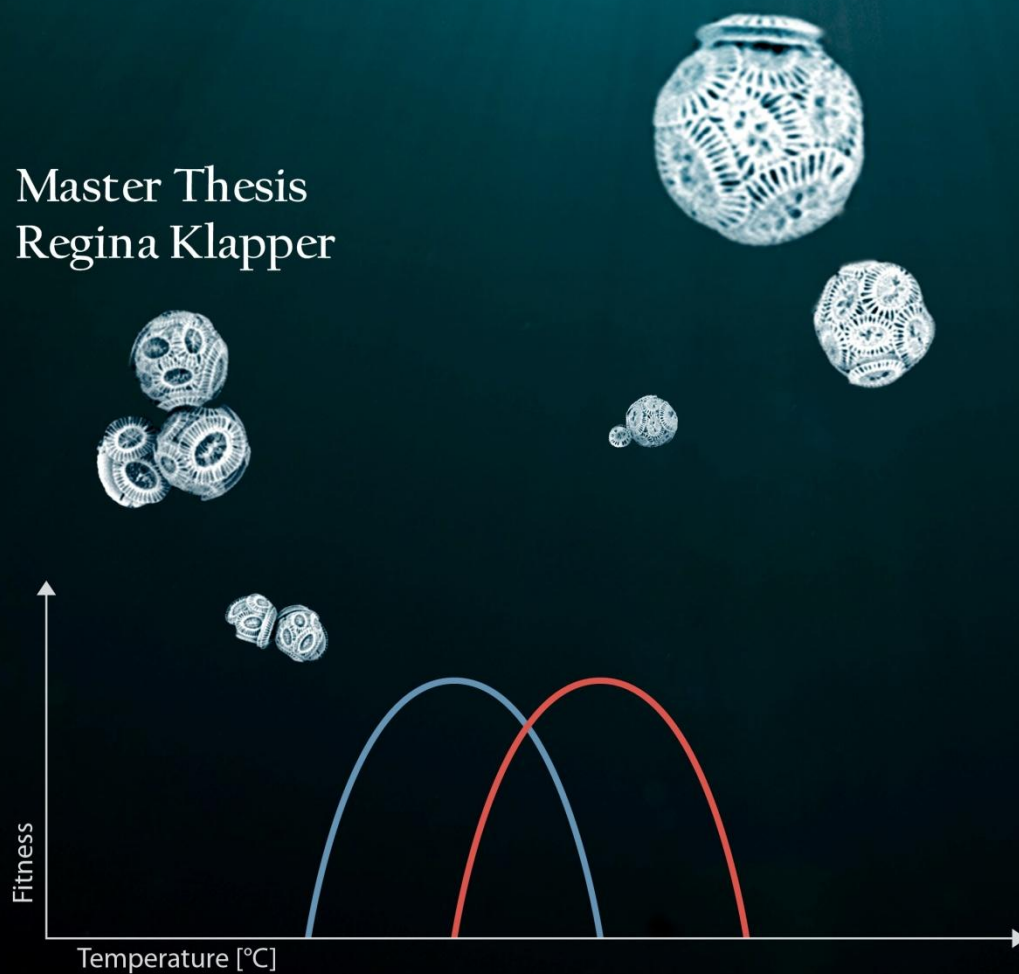


Local temperature adaptation of the widely distributed coccolithophore *Emiliana huxleyi*

Master Thesis
Regina Klapper



Master-Thesis in Biological Oceanography

By Regina Klapper

4311



GEOMAR | Helmholtz-Zentrum für Ozeanforschung Kiel,
EV Evolutionary Ecology of Marine Fishes

Düsternbrooker Weg 20, 24105 Kiel, Germany

Supervision:

Kai Lohbeck, *Evolutionary Ecology of Marine Fishes/ Biological Oceanography*

Departmental Supervision:

Prof. Dr. Thorsten Reusch, *Evolutionary Ecology of Marine Fishes*

Prof. Dr. Ulf Riebesell, *Biological Oceanography*

Kiel, October 2012

Table of Contents

Table of Contents	3
List of Figures	6
List of Tables	7
List of Equations	7
Abbreviations	8
Abstract	10
1. Introduction	11
1.1 <i>Emiliana huxleyi</i>	11
1.2 Role of biogeochemical processes in the ocean	12
1.2.1 Carbonate system of the ocean	13
1.2.2 Saturation state of the ocean	14
1.2.3 Biological and physical carbonate pump	15
1.2.4 Ballast hypothesis	16
1.2.5 Studies on ocean acidification and climate change	16
1.3 Adaptation and phenotypic plasticity	17
1.4 Aim of the study	21
1.5 Rationale	22
2. Material and Methods	23
2.1 Experiment	23
2.1.1 Experimental design	23
2.1.2 Culturing	24
2.1.3 Carbonate system	25
2.1.4 <i>Emiliana huxleyi</i> strains	25
2.1.5 Culture procedures	26
2.2 Growth rate/ Cell size counts	26
2.3 PAM chlorophyll fluorescence analysis	27
2.4 Scanning electron microscopy	29
2.5 Gene expression	30
2.5.1 RNA filtering and extraction	30
2.5.2 cDNA synthesis	31
2.5.3 Primer	31

2.5.4	RT-qPCR	32
2.5.5	qRT-PCR data analysis	33
2.6	Microsatellite analysis	33
2.6.1	DNA sampling and isolation	34
2.6.2	Microsatellite PCR	34
2.6.3	Fragment analysis	35
2.6.4	Analysis of Microsatellite data	36
2.7	Statistics	36
3.	Results	38
3.1	Population characteristics	38
3.1.1	Population structure	38
3.1.2	Morphotypes	39
3.2	Population comparison	40
3.2.1	Growth rates of populations	40
3.2.2	Chlorophyll fluorescence	42
3.2.3	Growth-Chlorophyll fluorescence-Size relationships	42
3.2.4	Gene Expression	44
3.3	Genotype variation and interaction	47
3.3.1	Growth rates of strains	47
3.3.2	Photosynthetic efficiency of PSII in single strains	49
3.4	Reaction norms of growth	49
3.4.1	Reaction norms over population	50
3.4.2	Reaction norms over strains	51
3.4.3	Reaction norms of Gene expression	52
4.	Discussion	54
4.1	Population structure and characteristics	54
4.2	Between-population differentiation	56
4.3	Within-population variation	59
4.4	Role of plasticity on marine phytoplankton	62
5.	Conclusions	64
	References	65
	A CaM and Hsp90	75
	B Histograms	76

Table of Contents

C Microsatellite Primers	78
D Carbonate System parameters	79
E Reaction norms gene expression	80
Acknowledgments	82
Declaration of Authorship	83

List of Figures

Fig. 1: Schematic diagram of the carbonate system in seawater	13
Fig. 2: Bjerrum plot	14
Fig. 3: Principle of reaction norm	20
Fig. 4: Experimental Design	24
Fig. 5: Chlorophyll fluorescence	28
Fig. 6: Modification of PHYTO-PAM fluorometer	29
Fig. 7: Coccolith morphology and denotation of elements	29
Fig. 8: Genetic diversity as distance	38
Fig. 9: Bar diagram	39
Fig. 10: SEM-images of Bergen	40
Fig. 11: SEM-images of Azores	40
Fig. 12: : Mean growth rates μ of populations	41
Fig. 13: Mean effective quantum yield of PSII of populations	42
Fig. 14: Correlation between growth rate [μ] and Φ PS II at treatment temperatures	43
Fig. 15: Relationships between Growth/Size and Temperature	44
Fig. 16: Treatment comparison of Gene expression	45
Fig. 17: Population comparison of Gene expression	46
Fig. 18: Growth rates in strains at 8°C	48
Fig. 19: Growth rates in strains at 22°C	48
Fig. 20: Effective quantum yield of PSII in single strains	49
Fig. 21: Reaction norm of populations over both temperatures	50
Fig. 22: Reaction norms of genotypes in Azores group	51
Fig. 23: : Reaction norms of genotypes in Bergen group	52

List of Tables

Tab. 1: Isolates used in experiment	26
Tab. 2: Candidate genes	31
Tab. 3: Dream Taq PCR Protocol.	35
Tab. 4: PCR Protocol.	35
Tab. 5: Optimized markers	35
Tab. 6: Nested ANOVA Gene expression.....	47
Tab. 7: ANOVA Genotype-by-environment interactions of gene expression	53

List of Equations

Equation 1: Total Alkalinity	14
Equation 2: Calcification	16
Equation 3: Growth rate μ	26
Equation 4: Effective quantum yield of PSII	27

Abbreviations

°C	Degrees Celsius
μ	Growth rate
ASW	Artificial seawater
ATPc/c'	Subunit c of the V ₀ sector of a Vacuolar H ⁺ -ATPase
CaCO ₃	Calcium carbonate
CaM	Calmodulin
CAX3	Cation/H ⁺ - exchanger 3
cDNA	Complementary DNA
CO ₂	Carbon dioxide
CO ₃ ²⁻	Carbonate
DIC	Dissolved inorganic carbon
DNA	Desoxyribonucleic acid
DOC	Dissolved organic carbon
<i>E. huxleyi</i>	<i>Emiliana huxleyi</i>
F _m '	Maximum fluorescence
F _v	Variable fluorescence
gDNA	Genomic DNA
GPA	Glutamic acid, proline and alanine-rich Ca ²⁺ - binding protein
G x E	Genotype-by-environment
H ⁺	Proton
H ₂ CO ₃	Carbonic acid
HCO ₃ ⁻	Bicarbonate
HPLC-H ₂ O	High-performance liquid chromatography water
Hsp	Heatshock protein
IPCC	Intergovernmental Panel on Climate Change
K ₁	First thermodynamic dissociation constant of the carbonate system
K ₂	Second thermodynamic dissociation constant of the carbonate system
mRNA	Messenger RNA
PAM	Pulse-amplitude modulated
PAR	Photosynthetically active radiation
pCO ₂	Partial pressure of carbon dioxide
pH	Potential hydrogenii
POC	Particulate organic carbon
PPFD	Photosynthetic photon flux density
PSII	Photosystem II
Q _A	Plastoquinone
RB	Small subunit of RuBisCO
RNA	Ribonucleic acid
-RT	Non-reverse transcribed RNA
RT-qPCR	Real-time quantitative polymerase chain reaction
RuBisCO	Ribulose-1,5-Bisphosphate Carboxylase/oxygenase
SEM	Scanning electron microscopy
SLC4	HCO ₃ ⁻ -transporter
STR	Short tandem repeats

TA, A_T	Total alkalinity
ΔF	Difference in fluorescence yield at maximal fluorescence (F_m) and the steady-state (F)
$\Phi_{PS II}$, $Y(II)$, $\Delta F/F_m'$	Effective quantum yield of PSII

Abstract

The impact of climate change on the ecologically and biogeochemically important coccolithophore *Emiliania huxleyi* has been a central question in phytoplankton research of the last decade. However, most studies focused on physiological responses while evolutionary processes were widely neglected. The present study investigated whether strains of *E. huxleyi* from different geographic origins are locally adapted to their respective average seawater temperature of 8°C from Bergen/Norway and 22°C from the Azores/Portugal. A reciprocal transplant experiment was conducted to find out whether differences between strains from different geographic origins are higher than among strains from the same origin. Using microsatellite analysis, I found restricted gene flow and could detect two distinct populations. Bergen strains grew faster than Azores strains at 8°C, while at 22°C both populations grew approximately equally fast. Photosynthetic efficiency was higher in Bergen strains at 8°C, and same in both populations at 22°C. While I found a good correlation of effective quantum yield of PSII responses and growth rates for 8°C showing a direct relationship between photosynthetic efficiency and growth, at 22°C no correlation was found, potentially due to light-limitation. There was a linear negative correlation between growth rate and cell size for all treatments, however cells from the Azores were generally bigger than cells from Bergen. Temperature-induced phenotypic plasticity of growth rate may be adaptive, as the Bergen strains maintained a higher fitness over the two exposed temperature conditions than the Azores strains. Moreover, variation in growth rates and effective quantum yield of PSII were always higher in both populations in their 'non-native' treatment, also indicative for adaptive phenotypic plasticity. Thus, strains from Bergen appear to have better abilities to buffer against environmental fluctuations than Azores strains, which is reasonable as Bergen strains encounter stronger temperature changes in their natural environment. Genotype-by-environment interactions were found in reaction norms of both growth rates and gene expression, so genotypes are affected differently by changing temperature conditions, indicating high standing genetic variation. My results suggest that high standing genetic variation and phenotypic plasticity may be important mechanisms for adaptation of natural *E. huxleyi* populations to changing environments and emphasize the importance of using more than one strain in studies aiming to investigate general responses of this species.

1. Introduction

Fossil fuel combustion increases the concentration of carbon dioxide (CO₂) in the atmosphere by an average rate of 1.9% per year (IPCC 2007). This rate, driven by anthropogenic emissions, is in an order of magnitude faster than the rate observed for the past millions of years (Doney and Schimel 2007). Consequently, climate changes rapidly with direct consequences like increasing temperatures and ocean acidification (Doney et al. 2009). Global mean temperature has increased by 0.8°C over the last 100 years (IPCC 2007). Since pre-industrial times, the pH of ocean surface water has dropped by 0.1 and is predicted to decrease further by 0.3-0.4 units until 2100 via elevated carbon dioxide uptake by the oceans (Orr et al. 2005). Currently, the CO₂ ocean uptake accounts for approximately one third of fossil fuel emissions (Sabine et al. 2004). Therefore, it is essential to understand how marine organisms are affected by climate change. Marine communities are biological networks, linked together through various biological interactions and are dependent on the performance of other species within the community (Doney et al. 2012). Climate change will affect organisms by causing habitat shifts, behavioral changes, altered phenology, and local extinctions (Reusch and Wood 2007). Aside from understanding how species will be impacted physiologically by climate change, knowledge on ecology, genetic evolution and phenotypic plasticity are also important in order to assess the composition and functionality of communities (Chevin et al. 2012). It is especially important to understand how keystone species will be affected. Coccolithophores are one of the most important phytoplankton groups as they are extremely abundant and have a major role in biogeochemical cycling (Paasche 2001). Despite the significance of coccolithophores for the global environments, their biodiversity, biogeography, ecology and evolution are still not well understood (Thierstein and Young 2004). Within this study, the question of whether the coccolithophore *Emiliana huxleyi* is locally adapted to its respective environment will be investigated by assessing the role of plasticity between genotypes within two temperature regimes according to their biogeographic origin.

1.1 *Emiliana huxleyi*

Although accounting only for one per cent of the global biomass, phytoplankton contributes to almost 45% of the world's primary production (Falkowski et al. 2004). The most abundant

calcifying phytoplankton species in the oceans is the coccolithophore *Emiliana huxleyi* (Westbroek et al. 1989). With the exception of polar regions with summer seawater temperatures of less than 2°C, *E. huxleyi* is nearly ubiquitous distributed (Buitenhuis et al. 2008). Blooms often occur in eutrophic regions (mostly following diatom spring blooms in temperate latitudes), but *E. huxleyi* also occurs in oligotrophic waters of subtropical gyres (Tyrrell and Merico 2004). Diatoms are typically dominant due to faster growth rates (Furnas 1990), but when silicate becomes limited diatoms cannot grow anymore and coccolithophores can become dominant (Egge and Aksnes 1992). The blooms that coccolithophores form impact climate on increased water albedo, DMS production, and changed oceanic CO₂ uptake (reviewed in Tyrrell and Merico 2004). Conditions of thermal stratification and high irradiance in phosphate-poor environments with excess of nitrate seem to promote blooms of *E. huxleyi* (Paasche 2001). Usually, diploid *E. huxleyi* cells are covered with small, calcified scales called coccoliths, which form a casing that is referred to as coccosphere (Westbroek et al. 1989). Coccospheres often consist of multiple layers of coccoliths. Morphological differences allow to distinguish morphotypes A, B, B/C, C, and R (Medlin et al. 1996, Young and Westbroek 1991). *E. huxleyi* has a haplo-diploid life cycle (Green et al. 1996).

E. huxleyi belongs to the class of Prymnesiophyceae which, together with the Pavlovophyceae, form the division Haptophyta (Jordan et al. 2004). Haptophytes are characterized by a 'haptonema', a flagellum-like appendage which differs from flagella in the arrangement of microtubules. In the fossil record coccolithophores appeared in the upper Triassic, reached their highest diversity in the Cretaceous and lost most of this diversity in a mass extinction during the Mesozoic/ Cenozoic boundary 65 million years ago (Thierstein and Young 2004). The species *E. huxleyi* diverged from *Gephyrocapsa oceanica* only 270 kyrs ago (Thierstein et al. 1977) and became the dominant coccolithophore 70,000 years ago (Bijma et al. 2001).

1.2 Role of biogeochemical processes in the ocean

Coccolithophores are among the most important calcifying organisms in the world's oceans due to their role in both ocean primary production and calcium carbonate deposition (Westbroek & Linschooten, 1989). About half of the modern calcium carbonate precipitation in the oceans is expected to be due to secretion of exoskeletons in coccolithophores

(Milliman 1993). They play a major role in controlling the carbonate chemistry and alkalinity in the surface oceans.

1.2.1 Carbonate system of the ocean

Atmospheric carbon dioxide concentrations are currently increasing to levels that have not been seen during the past 420,000 years (IPCC 2007). The oceans play an important role as they are one of the earth's major carbon sinks (Sabine et al., 2004). CO_2 fluxes are driven by both physical and biological processes: physically by molecular diffusion at the air/sea interface when there is a partial pressure difference of CO_2 across the interface, and uptaken CO_2 is then biologically converted to organic carbon compounds by ocean phytoplankton.

CO_2 dissolves in the surface ocean and reacts with sea water to form carbonic acid (H_2CO_3). This again dissociates to bicarbonate ions (HCO_3^-) and carbonate ions (CO_3^{2-}) under the release of hydrogen ions (H^+) (Fig. 1).

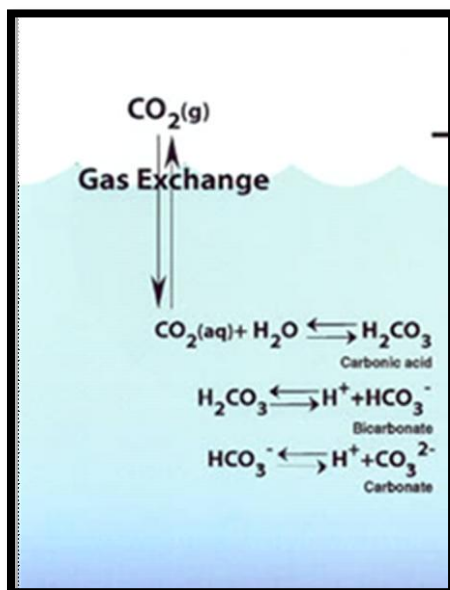


Fig. 1: Schematic diagram of the carbonate system in seawater. CO_2 is uptaken at the ocean-atmosphere boundary and dissociates into the different carbonate ion forms. In Feely et al. 2001.

In today's conditions, ions are in equilibrium with a distribution of approximately 90% bicarbonate, 10% carbonate, and 1% carbon dioxide, forming the dissolved inorganic carbon (DIC) pool. Seawater is buffered with respect to changes in hydrogen ions, but an increase of CO_2 will reduce the carbonate buffering capacity of the surface ocean. Through the larger fraction of dissociation of carbonic acid, more hydrogen ions are released and lower the pH. The Bjerrum plot (Fig. 2) illustrates the concentration of the carbon ions as a function of pH.

Dissociation constants pK_1 and pK_2 are temperature, salinity, and pressure dependent. The increase of CO_2 in the ocean will eventually lead to a shift of ion components by lowering the pH through increasing the release of hydrogen ions. pH is already lowered by 0.1 units compared to pre-industrial values and is predicted to decrease by another 0.3-0.4 units by the end of this century (IPCC 2007).

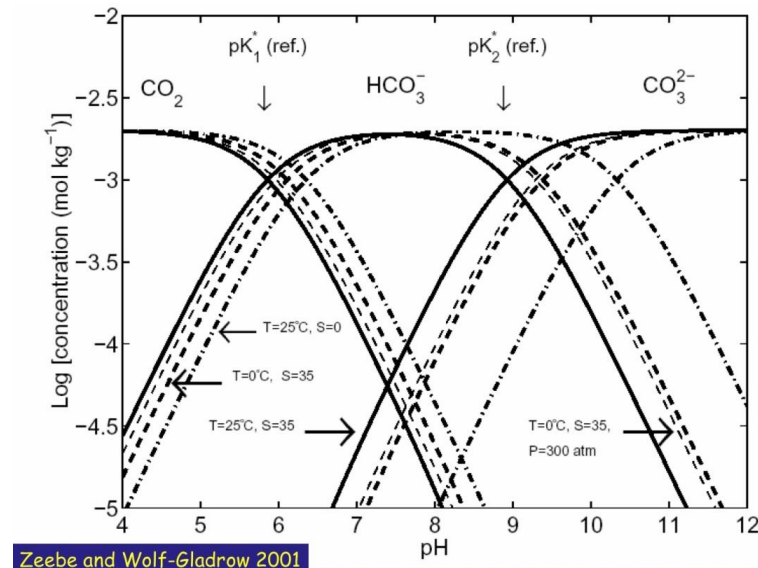


Fig. 2: Bjerrum plot. Concentrations of CO_2 , HCO_3^- , and CO_3^{2-} as functions of pH, dependent on salinity and temperature. CO_2 dominates for pH below pK_1 , CO_3^{2-} above pK_2 , and HCO_3^- in between (Zeebe and Wolf-Gladrow 2001).

Further, alkalinity is a natural buffer for carbonate ions in the ocean as it includes other acid-base species. Total alkalinity is the sum of all ions in the seawater and gives the excess amount of anions which can take up protons (Dickson et al. 1981), see Equation 1).

$$A_T = [HCO_3^-] + 2[CO_3^{2-}] + [B(OH)_4^-] + [OH^-] + [HPO_4^{2-}] + 2[PO_4^{3-}] + [SiO(OH)_3^-] + [NH_3] + [HS^-] + \dots - [H^+] - [HSO_4^-] - [HF] - [H_3PO_4] \quad (1)$$

1.2.2 Saturation state of the ocean

The degree of saturation in seawater of the two major $CaCO_3$ mineral forms, aragonite and calcite, is the ion product of the concentrations of calcium carbonate ions (dependent on in situ temperature, salinity, and pressure), divided by the stoichiometric solubility product (Feely et al. 2004). Currently, most of the oceans are supersaturated with respect to aragonite and calcite. The present-day surface saturation state is strongly influenced by temperature and is lowest at high latitudes, with minima in the Southern Ocean (IPCC 2007). Model simulations project that undersaturation will be reached in only a few decades (Feely

et al. 2004). Therefore, conditions harmful to high-latitude calcifiers could develop within decades, not centuries as suggested previously (Orr et al. 2005). However, since increasing atmospheric CO₂ concentrations lower oceanic pH by shifting carbonate ion concentrations, it is leading to a decrease of the saturation state with respect to calcium carbonate (Feely et al. 2004). Ocean acidification could thus possibly lead to undersaturation and dissolution of calcium carbonate in parts of the surface ocean during the 21st century, depending on the magnitude of increase in atmospheric CO₂ (Orr et al. 2005). Southern Ocean surface water is projected to become undersaturated with respect to aragonite at an atmospheric CO₂ concentration of approximately 600 ppm. This concentration threshold is largely independent of emission scenarios (IPCC 2007). Calcifying species have different degrees of sensitivity to these changes, because they can control biomineralization in a different degree (Doney et al. 2009).

1.2.3 Biological and physical carbonate pump

The carbon cycle is driven by the biological and the physical carbon pump. Firstly, CO₂ solubility in seawater increases with decreasing temperature, according to Henry's law (Weiss 1974). Atmospheric CO₂ is taken up by cold sea water in polar regions, especially in the Labrador Sea and Greenland Sea, where due to the higher density of colder water CO₂ sinks with the water masses into the deep sea (Sarmiento and Gruber 2006). The once exported CO₂ is upwelled again after approximately 1,000 years in which it was transported to the Southern ocean in a balanced ocean-atmosphere reservoir (Sarmiento and Gruber 2006). Currently, there is more CO₂ entering the ocean than leaving. Secondly, the biological pump consists of a soft and a counter-acting hard tissue pump. The soft tissue pump encompasses the carbon flux from the surface ocean to the ocean interior by interactions of vertically-structured pelagic ecosystems of the photic zone (Longhurst and Glen Harrison 1989). Organic carbon, produced by primary production is consumed by zooplankton or bacteria. A part of this organic carbon is transported vertically as particulate organic carbon (POC) and dissolved organic carbon (DOC). Most of it gets respired heterotrophically and is converted into dissolved inorganic carbon (DIC), which is finally upwelled again. Only a small fraction sinks into sediments. The DIC concentration is higher at depth than at the surface. The hard tissue, or calcium carbonate pump, on the other hand is mainly driven by calcifying organisms, where CO₂ gets released in the calcification process.



Consequently, the two biological pumps counteract each other with respect to release and uptake of oceanic CO₂, due to the different processes of photosynthesis and calcification.

1.2.4 Ballast hypothesis

The rain ratio is the ratio between export of organic carbon and calcium carbonate (Armstrong et al. 2001). It is important as the production and burial of both organic carbon and biogenic carbonate provides a potential sink for carbon. POC from the surface ocean is faster transported to the interior with ballast minerals such as carbonate biominerals because they increase the density (Honjo et al. 1982). Armstrong (2009) hypothesized that a large fraction of sinking particles must be ballasted to the seafloor or fluxes would not be that high. The transfer rate of POC into the deep sea determines how much atmospheric CO₂ is removed (Ittekkot 1993). Reduced calcification may lead to a decreased flux of organic matter (Armstrong et al. 2001). Thus, a decreased calcification in organisms would have major impacts on biogeochemical cycling (Zondervan et al. 2001).

1.2.5 Studies on ocean acidification and climate change

To understand biological and ecological consequences of climate change on *E. huxleyi*, many studies have been conducted that focus on the impacts of climate change on growth, calcification, and photosynthesis in order to predict whether this key species will be able to cope with the conditions of the future ocean (e.g. Riebesell et al. 2000; Zondervan et al. 2001; Zondervan and Riebesell 2002). Most studies found a decrease in calcification under elevated pCO₂ conditions, which could be a negative feedback on rising atmospheric pCO₂ (Zondervan et al. 2001). Mesocosm studies were conducted for simulating more realistic scenarios in which similar results were found (e.g. Buitenhuis et al. 2001, Delille et al. 2005, Engel et al. 2005). As climate change not only leads to ocean acidification, but also to increasing temperature, enhanced stratification, and consequently reduced nutrient access (Bindoff et al. 2007), studies on interactions between several parameters have become of interest. *E. huxleyi* has been found to be sensitive to both changing pCO₂ and temperature (De Bodt et al. 2010). Also interactive effects of increased pCO₂, temperature and irradiance were detected (Feng et al. 2008).

Differential results were found in studies of coccolithophores on ocean acidification, e.g. Langer et al. (2006) did not find linear CO₂-related responses in the calcification response

previously found in two coccolithophore species, and the two investigated species responded differently to CO₂ changes. In a later study, different physiological responses in *E. huxleyi* were detected to be strain-specific to elevated pCO₂ conditions (Langer et al. 2009). These strains originated from different parts of the ocean. Recent work discovered a distribution of differently calcifying strains in the world's oceans with an overall trend of decreasing calcification with increasing pCO₂ as has been found in culture based studies earlier. Notably, an unexpected highly calcified morphotype could be found in an upwelling region off Chile, in which the trend would have suggested the opposite due to its carbonate chemistry (Beaufort et al., 2011). It was argued these differences in strains must have genetic bases (Langer et al., 2009).

1.3 Adaptation and phenotypic plasticity

Due to the role of calcifying marine microorganisms on marine biogeochemical cycles, an important question is how biogeochemical cycles will be affected by changing environmental conditions and whether species responses will buffer the changes in biogeochemical cycles (Chevin et al. 2012). Studies on organism's responses to climate change have nearly exclusively been short term physiological studies, neglecting the potential for adaptation to changing conditions (Hofmann et al. 2010). Studies on the effects of climate change on geographically widespread species should also take into consideration genetic, morphological, and physiological variability (Cook et al. 2011). Additionally, genetic evolution and phenotypic plasticity could affect the functionality and composition of communities (Chevin et al., 2012). Therefore, key aspects in predicting future ocean conditions are ecological and evolutionary processes. Marine microorganisms are expected to be the first group to respond evolutionary to environmental changes (Gabriel and Lynch 1992). In selection experiments, *Chlamydomonas* grown for about a thousand generations in high CO₂ failed to show a direct adaptive response to increased pCO₂ conditions (Collins and Bell 2004). Only recently it has been shown that strains of *E. huxleyi* adapted to high pCO₂ conditions calcified more and had higher growth rates than control strains (Lohbeck et al. 2012). Langer (2009) showed there are differences between strains of *E. huxleyi* from different origins in the ocean. However, whether variation between strains from different sites is higher than the variation of strains from the same origin site has yet to be clarified (Wood and Leatham 1992). The question is whether signs of adaptation to certain environmental factors can be detected in the ocean. Another possibility would be the

ubiquitous dispersal of marine microbial species, depicted as the 'everything-is-everywhere' hypothesis (Finlay 2002, Finlay and Clarke 1999). The hypothesis implies that there is no biogeography for microbes: they can survive in a wide range of environments, but grow differently well in various environments. Phytoplankton are most likely not evenly distributed in the heterogeneous oceans because they are passive drifters and ocean currents form frontal boundaries (Palumbi 1994). Because they often encounter dramatic temporal fluctuations in environmental conditions, their physiological functioning is typically buffered against such environmental heterogeneity (Reusch and Boyd, 2012 submitted). As a consequence of ocean boundaries, gene pools get disrupted and the local adaptation of populations evolves, leading to physiological and morphological differentiation for specialization to the respective environment (Medlin 2007). Populations can either adapt through selection on new, beneficial mutations or through already existing genetic variation, where the latter is considered to be faster (Barrett and Schluter 2008). Standing genetic variation is the presence of more than one allele at a locus in a population (Barrett and Schluter 2008). A high standing genetic diversity in phytoplankton populations is likely (Medlin et al. 1996, Ryneerson and Armbrust 2000). In a *Ditylum brightwellii* bloom a high genetic diversity, obtained using microsatellite markers, was retained and most of the daily sampled cells were found to be genetically distinct from each other (Ryneerson and Armbrust 2000). How genotypic diversity is maintained within populations remains a central question in ecology (Rainey et al. 2000). So far, a leading explanation for the maintenance of this diversity is that temporal fluctuations exert selection pressure on genotypes in seasonally changing habitats (Gsell et al. 2012). Phenotypes are controlled both by the genotype and the environment (Bradshaw 1965). Phenotypic plasticity might be an adaptive strategy that allows genotypes to cope with different environmental conditions and therefore can reflect genetic diversity (De Jong 1990). Phenotypic plasticity is defined as the ability of a genotype to change the phenotype in different environments (Bradshaw 1965). If individuals can cope with changing conditions through plasticity, that might dampen the effects of natural selection and hence slowing genetic divergence (Crispo 2008). Phenotypic plasticity and genotype-by-environment interactions can be illustrated via conduction of reaction norms (Woltereck 1913). Reaction norms show the response function characteristics of single genotypes (Parejko and Dodson 1991) and the plasticity of a trait across environments (Schlichting and Pigliucci 1995). There is a genotype x environment

interaction when the phenotypic response of a genotype varies across environments and when different genotypes perform differently across these environmental conditions (De Jong 1990). Response differences between genotypes can be statistically identified as genotype-by-environment (G x E) interaction by variance analysis (Bell 1991). Graphically, differences in genotypic reaction norms can be shown when slopes are non-parallel or cross each other (Gsell et al. 2012), where each line represents the phenotypic response in a certain environment of one genotype (Fig. 3, Pigliucci 2005). More plastic genotypes have phenotypes that change faster with the environment, and thus having a greater slope (Chevin et al. 2012). Models revealed that, in spatial heterogeneity, genotypes are selected for higher plasticity (Via and Lande 1985). Further, phenotypic plasticity can evolve by natural selection (Scheiner 1993). Plasticity allows for the colonization and success of habitats and other forces lead to restricted gene flow, which eventually leads to local adaptation (Agrawal 2001). Plasticity is considered to be adaptive when plasticity in functional traits enhances survival or reproduction (Richards et al. 2006). Demographic models gain explanatory power by including rapid phenotypic responses (Ezard et al. 2009, Ozgul et al.). In Lohbeck's experiment (2012), differences occurred between strains: while in a single-strain experiment strains evolved by selection of new beneficial mutations, in a multiclone experiment selection of on pre-adapted genotypes was found. Additionally, in a study on *Chlamydomonas*, relative fitness was found to be sensitive to particular combinations of environmental factors (Bell 1991). Hence, the question arises whether strains of *E. huxleyi* are differently affected by environmental changes.

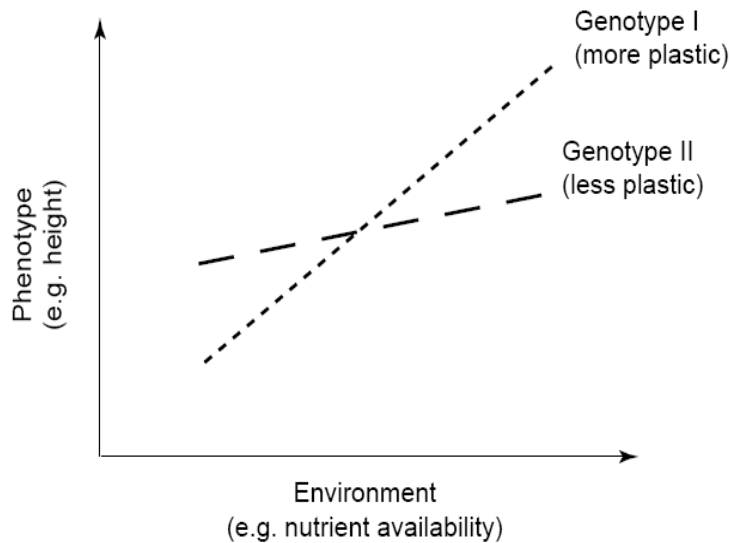


Fig. 3: Principle of reaction norm. Reaction norms of two genotypes are shown, where genotype I is more plastic because the phenotype change is greater than of genotype II. X-axis: Environmental condition, y-axis: phenotypic response (in Pigliucci 2005).

Gene expression analysis makes phenotypes which can normally not be detected visible. Gene expression may facilitate population persistence and contribute to genetically- based reproductive isolation (Pavey et al. 2008). Variation in gene regulation might be a critical determinant of phenotypic variation (Reusch and Wood 2007). Gene expression itself can be plastic and a result of responses to environmental changes, as such they can show different levels of transcriptional regulation in different environments as a reaction norm (Aubin-Horth and Renn 2009). In model organisms, different genotypes can have different norms of gene expression (Landry et al. 2006, Li et al. 2006). However, it would be important to show this for ecological more important species. Studies on gene expression in *E. huxleyi* were conducted mainly to understand cellular processes, especially related to calcification (Mackinder et al. 2011, Quinn et al. 2006, Richier et al. 2011, Richier et al. 2009). Other studies focused on metabolic processes in the context of nutrient availability (e.g. Bruhn et al. 2010, Kaufman 2007). Differences could be found in regulating genome expression, proteome maintenance, and metabolic processing of calcified and non-calcified strains (Rokitta et al. 2011).

Temperature is one of the major factors influencing physiological processes and metabolic rates (Beardall and Raven 2004). Growth rates have been found to be consistent with the biogeographical distributions of different coccolithophore species. In a study by Buitenhuis

et al. (2008), four different species were grown in a temperatures range from 6 to 25°C. *E. huxleyi* was the only species that grew at all temperatures. Brand (1982) found strains of *E. huxleyi* and *Gephyrocapsa oceanica* from different regions to have growth optima at different temperatures, thus strains are likely to be temperature-selected and show genetic variability. A study by Conte et al. (1998) also found differences in *E. huxleyi* and *G. oceanica* strains' growth rates of over a range of 6-30°C to be consistent with their cold and warm water origins. Notably, a study on temperature responses of a harmful bloom alga, *Fibrocapsa japonica*, showed that strains from three different climate regions show different degrees of adaptation to their native environment (De Boer et al. 2005).

1.4 Aim of the study

This study aims to investigate whether *Emiliania huxleyi* strains are adapted to the temperature environment of their geographic origin by comparing mean fitness of populations and whether phenotypic plasticity has evolved. Additionally, the magnitude of strain-specific variation within a population should be investigated. As *E. huxleyi* was found to be able to grow at a broad range of temperatures, it should be highly plastic. Reaction norms were conducted to see whether there are no differences in responses of genotypes to the same environmental changes or whether there are genotype-by-environment interactions. However, aside from the need for more information of physiological responses to the changing environment, molecular mechanisms are still poorly understood. So far, I could not find any study investigating gene expression on temperature changes in *E. huxleyi*. Additional analysis on gene expression may help to understand relations of transcriptional regulation and the corresponding phenotype.

Hypotheses:

1. Strains of *E. huxleyi* are adapted to the average seawater temperature of their geographic origin. Strains are performing best in their naturally encountered temperature and will be less fit when grown in other temperatures.
2. Photosynthetic efficiency of PSII is higher when strains are grown in their native temperature environment compared to when they are grown in their non-native environment.
3. Gene expression of candidate genes is temperature-and population dependent. In the non-native temperature, genes involved in stress-responses are up-regulated.

4. Due to the high genetic diversity found in natural phytoplankton populations, there will be genotype-by-environment interactions illustrated. As higher plasticity is favoured in temporal or spatial heterogeneity (see Via and Lande 1985), Bergen strains will show higher plasticity because they should be used to higher seasonal temperature fluctuations.
5. Microsatellite analysis will reveal genetic differentiation between the Azores and Bergen population.

1.5 Rationale

As measuring fitness of local and nonlocal genotypes across contrasting habitat types can provide indirect evidence for the potential of adaptive evolution (Bradshaw and Holzapfel 2007, Reusch and Wood 2007), strains from a northern (Bergen, Norway) and a southern location (Faial, Azores, Portugal) were kept at their approximate average temperature regime and the respective other one, denoted in this study as 'native' and 'non-native'. Growth rates μ were measured as a fitness proxy, as well as mean cell size and effective quantum yield of PS II ($\Delta F/F_m'$), used here as indirect measurement for photosynthetic efficiency at culturing conditions. These parameters were first analysed on the population level in order to investigate possible differences between populations. Thereafter, responses were compared at the strain level for distinguishing variation between strains. Finally, the individual responses were used to investigate genotype-by-environment interactions by applying reaction norms. To get insights into the 'molecular phenotype', gene expression was conducted with candidate genes using real-time quantitative polymerase chain reaction (RT-qPCR). In order to detect the population structure, microsatellite analysis was performed. To verify that all strains belong to the same morphotype, scanning electron microscopy (SEM) images were taken.

2. Material and Methods

Strains of *Emiliana huxleyi* originating from a northern and a southern location were used to test for local temperature adaptation. Before conducting an experiment, strains from stock cultures were first tested for genetic relatedness using microsatellite markers, and approximate growth rates at different temperatures were determined in a pre-experiment. In the main experiment growth rates, mean cell sizes, and effective quantum yield of PSII were measured. Furthermore, gene expression analysis of candidate genes was accomplished via real-time quantitative polymerase chain reaction (RT-qPCR).

2.1 Experiment

2.1.1 Experimental design

Strains of *E. huxleyi* were isolated from Faial/ Azores, Portugal (where no dense blooms occur) in May/ June 2010 by Lena Eggers and Bergen, Norway (during a bloom) in May 2009 by Kai Lohbeck. The strains were grown under warm (22°C) and cold conditions (8°C) which represent the approximate average temperature of their origin. Stock cultures were kept at 15°C in tissue culture flasks (Sarstedt, Germany) with green ventilation caps, under approximately 120 photons/ m²/ sec PAR and a 13/11 light/dark cycle.

Experimental temperatures were determined using average surface temperatures of the locations the strains originated from (Bergen: 10.2 °C [weatheronline.co.uk], Cape Verde, Praia 23.8 °C [sea-temperature.com]). To obtain the same temperature difference from stock culture conditions of 15°C, a difference of ±7°C was chosen resulting in experimental temperatures of 8 and 22°C. Each strain was replicated five times to measure variation not only between strains and locations but also within the strains. If a response in the experiment was detected which can be related to the natural origin of the strains, it is stronger than the adaptation to the laboratory conditions.

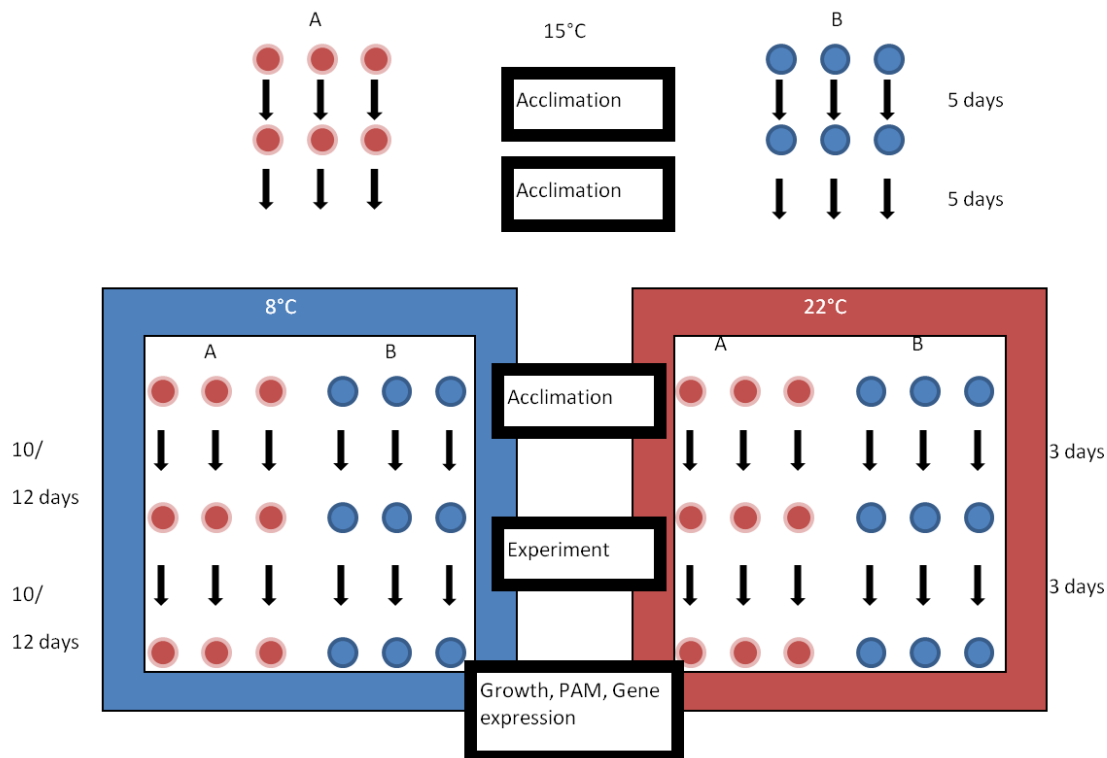


Fig. 4: Experimental Design. Strains A= Azores in red, B= Bergen in blue were kept at 15°C for two batch cycles, $n=5$. After transfer to experimental temperature, they were acclimatized for another batch cycle to 8 and 22°C, respectively. Thereafter, the test cycle was performed. Growth rate, cell size, and chlorophyll fluorescence were measured, and RNA filters were taken. The time in days of each batch cycle is indicated.

Fig. 4 illustrates the experimental design. Six strains from each location were chosen. As space was limited in the climate chambers, the experiment had to be split into two parts performed one after the other. Here, treatment temperatures were altered between the chambers to exclude effects of the climate rooms. Strains were inoculated from stock cultures into the experimental culturing bottles and acclimatized for two batch cycles to the experimental conditions at 15°C. After that, they were transferred into another temperature acclimation cycle at treatment temperatures in order to ensure acclimation. After the test cycle measurements of growth rates, cell sizes, chlorophyll fluorescence, and RNA filters were taken.

2.1.2 Culturing

Flasks were kept in a light cabinet with a photon flux density of $160 \pm 10 \mu\text{mol m}^{-2} \text{s}^{-1}$ under a 16:8 L/D cycle. In order to determine the positions in the light cabinet of desired photon flux density, a Lightmeter in connection with a US-SQS/L Submersible Spherical Micro Quantum Sensor (both Walz, Germany) was used. There was no temperature effect on the light

intensity of the fluorescence tubes. The cultures were rotated ten times twice a day to avoid sedimentation of the cells, and their positions were changed in a systematic manner in the light cabinet to avoid possible position effects.

Cultures were grown in sterile filtered (0.2 μm Whatman Polycap 75AS, GE Healthcare, UK) artificial seawater (ASW), bottled in 250 mL (Schott Duran, Germany) square flasks filled with a minimum headspace of approximately 1 mL to keep air-water- CO_2 -exchange small. ASW included 64 $\mu\text{mol kg}^{-1}$ nitrate, 4 $\mu\text{mol kg}^{-1}$ phosphate according to Redfield (1963), trace metals and vitamins adapted from f/8 (Guillard and Ryther 1962), 10 nmol kg^{-1} selenium, 2 mL kg^{-1} sterile filtered North Sea water (see Lohbeck et al. 2012). After setting up the carbonate system, ASW was filled in the culture bottles using a sterile silicon hose. All culture work was done under the clean bench with sterile materials. Bottles were stored at treatment temperature until inoculation of the algae. After usage, they were cleaned in the dishwasher without any dish detergents, washed with Milli-Q water, and finally autoclaved.

2.1.3 Carbonate system

For the carbonate system setup, 2380 $\mu\text{mol bicarbonate kg}^{-1}$ ASW were added (Merck, Germany), yielding the total alkalinity (TA) and dissolved inorganic carbon concentrations of 2380 $\mu\text{mol kg}^{-1}$. The preparation of the ASW was followed by an aeration of controlled CO_2 gas with 400 $\mu\text{atm pCO}_2$ for 48 hours. Aeration was done under a target treatment temperature in a climate chest. DIC samples were taken from the ready-made culture media of each batch cycle and were measured colorimetrically (Dickson et al. 2007) using a SOMMA autoanalyzer. Total alkalinity was measured from all treatments by open-cell acidimetric titration using a Metrohm Basic Titrino 794. DIC and TA measurements were used to calculate CO_2 partial pressure in the artificial seawater using the software CO2SYS (Lewis and Wallace 1998) with solubility constants of Roy et al. (1993) (Values, see Appendix). Average pCO_2 levels per treatment before inoculation were 371.8 μatm (± 37) in 15°C, 331.8 μatm (± 20) in 8°C, and 337.1 μatm (± 14) in 22°C.

2.1.4 *Emiliana huxleyi* strains

Six *E. huxleyi* strains for each site were taken from stock cultures, inoculated into 250 mL (Schott Duran, Germany) square flasks and brought into the climate cabinets. Strains used are listed in the below table Tab. 1.

Tab. 1: Isolates used in experiment. Labels of the strains during the experiment and name of stock culture are given.

Bergen	Cap Verde
B1: 75	A1: M23
B2: 62	A2: M22
B3: 41	A3: M21
B4: 85	A4: M19
B5: 63	A5: M13
B6: 17	A6: M10

2.1.5 Culture procedures

For inoculation, volumes containing 100.000 cells were transferred from the old culture flasks into the new flasks. This equates to a concentration of 321 cells/ mL. To limit changes in carbonate chemistry due to algal growth, cultures were transferred after approximately 8 generations into the next batch cycle before the cell concentration reached 100.000 cells/ mL. A maximum DIC draw down of 9.3% was calculated based on final cell numbers and cellular carbon quotas from *E. huxleyi* following the approach of Bach et al. (2011). In a pre-experiment, approximate growth rates of the cultures were determined so as to estimate the period of growth until inoculation. The duration of a batch cycle was five days in the 15°C treatment, 3 days in the 22°C treatment and 10 (Bergen) /12 (Azores) days in the 8°C treatment.

2.2 Growth rate/ Cell size counts

Cell numbers and mean cell sizes were assessed with the Z2 Particle and Size Analyzer (Beckmann Coulter, United States). Cell numbers were counted in triplicate for each replicate and always conducted at the same time of the day, two hours after light in the cabinets was switched on. Before counting, bottles were rotated to homogenize cell density. Exponential growth rates (μ) were calculated for each replicate after the following formula:

$$\mu = \frac{\ln(t_{fin}) - \ln(t_0)}{d} \quad (3)$$

Here t_0 and t_{fin} represent the cell numbers at the beginning and the end of a growth interval, and d is the time in days between these two counts.

2.3 PAM chlorophyll fluorescence analysis

Measurements on chlorophyll fluorescence can provide information on various photosynthetic processes and can be used as an indicator for photosynthetic electron transport in intact leaves and algae cells, and provide information on the functional state of the photosystem II (PSII) (Krause and Weis 1991). Furthermore, they are useful tools in the detection of various stress responses in plants (Krause and Weis 1984). Excitation energy cannot only be used photochemically, but also be transformed to heat, or transferred as emission by fluorescence (Krause and Weis 1991). As such, the rate of photochemical energy conversion and the rate of non-radiative energy dissipation are the two major factors causing changes in fluorescence yield (Schreiber et al. 1994). Stress reduces the photosynthetic efficiency and the amount of fluorescence will increase rapidly (Krause and Weis 1991). Chlorophyll fluorescence can be measured with the saturation pulse method (Schreiber et al. 1987). Fig. 5 is showing the principle of the method. In the saturation pulse method a sufficiently strong light pulse is given which reduces Q_A fully. Thus, photochemical fluorescence quenching becomes suppressed while the remaining quenching is non-photochemical and fluorescence (Bradbury and Baker 1981). An actinic light pulse is given to measure the parameters F_0 , F , F_m or respectively F_m' in dark- or light-adapted plants. The minimal fluorescence yield, F_0 , is observed when all reaction centres are open, this means Q_A (plastoquinone D2- subunit) is fully oxidized. In contrast, when all centres are closed (Q_A is fully reduced), a maximal fluorescence yield, F_m , is reached. The difference between F_0 and F_m is called variable fluorescence, F_v . By illuminating plants with actinic light, Q_A reduction rate is initially higher than the rate of reoxidation by plastoquinone and by PS I activity and later adjusting to a steady-state. As a result the fluorescence rise is correlated to the exhaustion of the PS II acceptor pool (Murata et al. 1966). The potential maximal PS II quantum yield can be calculated with the ratio $(F_m - F_0)/F_m = F_v/F_m$ (Butler 1978). It can be used as an indicator for the health status of a dark-adapted plant. An alternative, for light-adapted plants, is the effective quantum yield of PSII:

$$Y(II) = \frac{F_m' - F}{F_m'} = \Delta F / F_m' \quad (4)$$

Where F is the steady-state fluorescence, F_m' the maximum fluorescence, and ΔF is the difference in fluorescence yield at maximal fluorescence (F_m) and the steady-state (F). This

measurement estimates changes in the quantum yield of non-cyclic electron transport, giving a measure of photochemical utilised excitation energy (Genty et al. 1989).

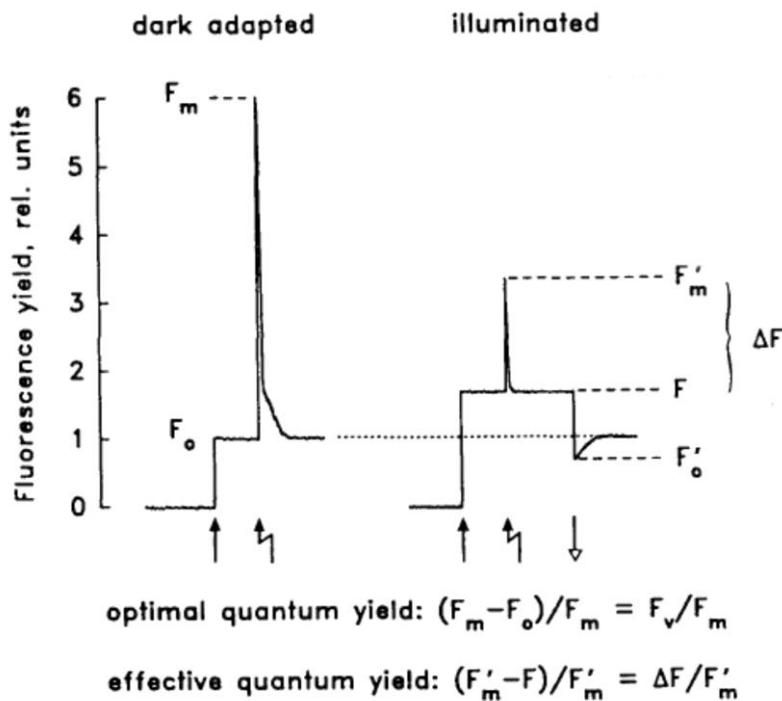


Fig. 5: Chlorophyll fluorescence. Resulting from the pulse amplitude modulated fluorometry measurements. Within my study, the effective quantum yield of PSII was measured (modified, after Schreiber et al., 1994). Therefore, a light pulse at the light intensity of culturing conditions, followed by a saturation pulse was given to measure the photosynthetic efficiency of PSII.

For the measurements a PHYTO-PAM fluorometer and Optical Unit ED-101US/MP with the measuring adapter PHYTO-US (Walz, Germany) was used. As dark-adaptation was not possible due to the location of the PHYTO-PAM next to a culture bank, samples were kept light-adapted. Samples were individually brought from the climate room to the fluorometer to assure that no light acclimation occurred to the changed light conditions. As samples should be kept at their treated temperature, strains from 22°C could be measured at room temperature, while the PHYTO-PAM was cooled for the 8°C samples. Therefore, a Styropor® box was built around the PHYTO-PAM and brought to $8 \pm 2^\circ\text{C}$ by addition of thermal packs (Fig. 6). Actinic illumination of $140 \mu\text{mol m}^{-2} \text{s}^{-1}$ was applied for 30 sec, followed by a saturation pulse to determine the effective quantum yield (Yield = dF/F_m) by four channels measuring at different excitation wavelengths (470 nm, 520 nm, 645 nm and 665 nm). From these, the mean was calculated for each sample.

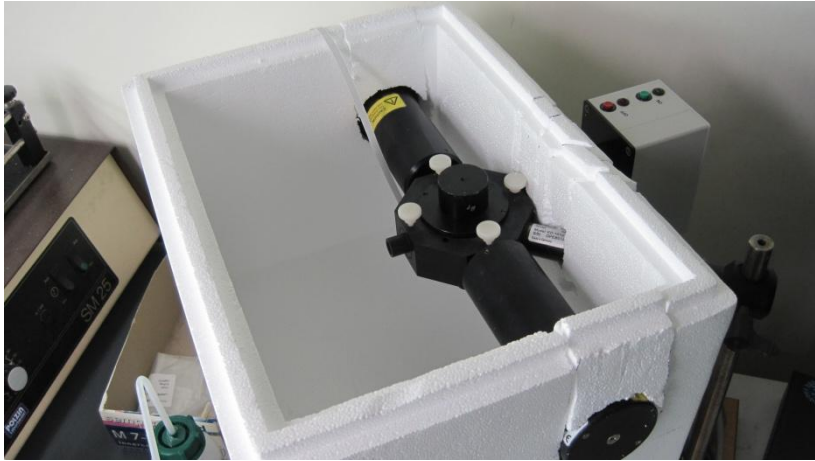


Fig. 6: Modification of PHYTO-PAM fluorometer. Samples from 8°C should be kept at this temperature. Therefore, a box of Styropor® was built around the PHYTO-PAM fluorometer and filled with thermal packs until target temperature was reached.

2.4 Scanning electron microscopy

For purposes of comparison, it was important that all strains were the same morphotype, because they are genetically different (Medlin et al. 1996), and are distinct in several characteristics, e.g. growth (Paasche and Klaveness 1970). Because of the origin from which they were isolated, cells were expected to be morphotype A. Properties of Type A are: liths are medium-sized with 3-4 μm , distal shields are robust, and central area elements curved (see Fig. 7).

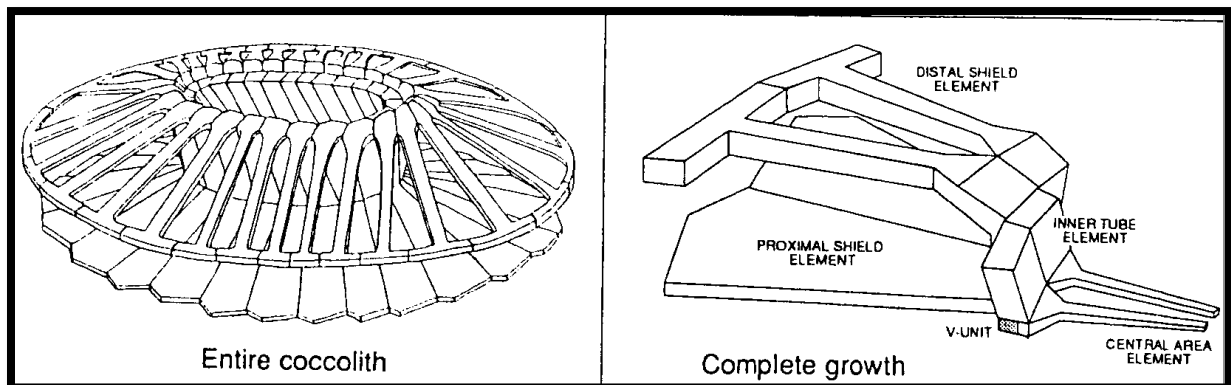


Fig. 7: Coccolith morphology and denotation of elements. Characteristics of coccolith morphology were used for determination of the strain morphotypes (In Paasche 2001).

To determine the morphotypes of the cultures, strains were checked by scanning electron microscopy (SEM). Therefore, approximately 200,000 cells were gently filtered with a pressure of ≤ 50 mbar on polycarbonate filters (Polycarbonate Track-Etch Membrane, 0.2 μm Sartorius, Germany) from the 22°C temperature regime. Filters were stored in small glass-

dishes and dried at room temperature. SEM-images were compiled on a Phenom G2 pure desktop SEM (Phenom World, Netherlands) at magnifications of 3500-7000 times.

In strain B1/75, most of the cells had no coccoliths. As the resolution of the scanning electron microscope was not high enough, it could not be determined whether the observed cells were a contamination by a different species or if the cells partly lost their ability to calcify. Therefore, the strain was excluded from any further analysis.

2.5 Gene expression

Gene expression is a rapid technique to quantify amounts of mRNA (Mullis et al. 1986). By using a reverse transcription assay, specific mRNA expression from any type of biological sample can be quantified (Reviewed in Bustin 2000). RT-qPCR consists of three steps: 1. Conversion of RNA into cDNA with reverse transcriptase, 2. cDNA amplification in a PCR, and 3. Detection and quantification of amplification products in a real-time PCR (Gibson et al. 1996). For the real-time PCR, fluorescent reporter dyes are used to combine the amplification and detection steps in a PCR (Higuchi et al. 1992, Higuchi et al. 1993). The resulting fluorescence signal in the PCR is directly proportional to the amount of cDNA produced in each cycle during the exponential phase of the reaction. Single reactions are characterized by the PCR cycle at which the fluorescence rises above a certain threshold cycle, named C_T (in Nolan et al. 2006).

RT-qPCR was applied to quantify the gene expression of several candidate genes which are potentially affected by temperature.

2.5.1 RNA filtering and extraction

Approximately 250 mL of the cell cultures were filtered with a Whatman® filter cyclo pore track etched membrane, 0.8 μm (GE Healthcare, UK) at ≤ 100 mbar. Filters were washed with 500 μL RNeasy lysis buffer (QIAGEN, Germany), cell suspensions were pipetted into 1,5 mL Eppendorf tubes and were placed on ice for several hours until a pellet had formed, and then frozen at -20°C .

RNA extraction was done using the RNeasy mini kit animal cells (QIAGEN, Germany). RNeasy lysis buffer samples were thawed on ice. 500 μL HPLC- H_2O were added to each sample and centrifuged for 5 min at full speed in a 5424 Centrifuge (Eppendorf, Germany), and the supernatant was removed. Lysis buffer (350 μL) containing β -Mercaptoethanol (1:100) was added. Samples were vortexed for 30 sec, followed by a 3 min sonification (Sonorox Digital

10P, Bandelin, Germany), and were vortexed again for 30 sec. 350 µL 70% ethanol were added and the samples were bound on columns by 15 sec of centrifugation at 10,000 rpm (Eppendorf, Germany). After several washing steps according to the protocol, the RNA was eluted with 40 µl RNase-free water and stored at -80 °C. RNA quantity was measured with Qubit 2.0 Fluorometer (Invitrogen, Life technologies, Germany).

2.5.2 cDNA synthesis

200 ng RNA were added to 15 µL HPLC-H₂O. Potential contaminations by genomic DNA were removed by the addition of 2.5 µL/reaction gDNA Wipeout Buffer 7x. The reaction was incubated for 2 min at 42 °C and after that, kept on ice. A non-reverse transcribed RNA (-RT) control was taken to ensure that gDNA wipeout was successful. The samples were then reverse transcribed into cDNA by the addition of the Master Mix which contained a mixture of oligo-dT and random primers. After an incubation time of 15 min at 42 °C, the reagents were inactivated at 95 °C for 3 min. The product was kept on ice, and 2 µL of the sample were transferred on a new plate for a dilution of 1:50. The pure cDNA, the dilution, and the control were stored at -80 °C.

2.5.3 Primer

Primers of candidate genes are taken from different studies (Kaufman 2007, Mackinder et al. 2011, Richier et al. 2009, Tab. 2). Primers were chosen to be potentially temperature-impacted: Genes involved in calcification, photosynthesis, general membrane potential maintenance, and stress response. Efficiency curves were generated with pooled cDNA from several samples of different treatments. For standard curves, the dilution started with 0.1, and was further diluted in 1:3 steps until 1:2430. Only primers were used which had an R² of >0.95 and an efficiency of 90-110 were used.

Tab. 2: Candidate genes. Tested candidate genes are listed with the primer sequence and the publication of the primers are named.

Gene name	Full name/ Function	Primer sequence	Author
Act	Actin	GAC CGA CTG GAT GGT CAA G GCC AGC TTC TCC TTG ATG TC	Mackinder et al., 2011
PK	Pyruvate kinase	ATG GAC GCA AAG GGA ATG CGA GGA TCT CGT CAA TGT TC	Mackinder et al., 2011
CAX3	Cation/H ⁺ Exchanger	CTC CTC TGC GTC TTT GCA T GAG GGC GGT GAT GAG GTA	Mackinder et al., 2011

gammaCA	Gamma carbonic anhydrase	TCT CCG CCT CAG TCA ACC AAG TTG TCG ACT GTG CAA CC	Mackinder et al., 2011
ATPc/c'	Subunit c of the V0 sector of a Vacuolar H ⁺ -ATPase	TAC GGC ACT GCA AAG TCT G ACG GGG ATG ATG GAC TTC	Mackinder et al., 2011
GPA	Glutamic acid, proline and alanine rich CA ²⁺ binding protein	AGG CCT TCT CCA GCA TCA T GTT CAG CGT GCT CTC CGA G	Richier et al., 2009
SLC4	HCO ₃ ⁻ —transport, AEL1 involved in carbon transport and pH Homeostasis	TTC ACG CTC TTC CAG TTC TC GAG GAA GGC GAT GAA GAA TG	Mackinder et al., 2011
RB	Small subunit of RuBisCO, Photosynthesis	CAA TCG GTC ACC CAG ATG GTA GCG ATA TAA TCA CGG CCT TCG	Mackinder, personal communication
Alpha Tubulin	Housekeeping gene	GCA TCG CCG AGA TCT ACT C TCG CCG ACG TAC CAG TG	Mackinder, personal communication
Hsp70	Heat shot protein	GAA GAT ACC CCA CCA CCG AGT CGA CAA GCC	Kaufman, 2006
Hsp90	Heat shock protein	CCG TCG GTC GAG AAT GCA CCG TGT ACT CGT	Kaufman, 2006
CaM	Calmodulin, Signaltransduction, Calcium sensor	ATC GAC TTC CCC GAG TTC T CGA GGT TGG TCA TGA TGT G	Richier et al., 2009
Alpha CA	Carbonic anhydrase	AGA GCA GAG CCC TAT CAA CA TCG TCT CGA AGA GCT GGA A	Mackinder et a., 2011

2.5.4 RT-qPCR

The 20 µL reaction contained 10 µL SYBR green, 0.8 µL forward primer, 0.8 µL reverse primer (final concentration 200 nM), 4.4 µL HPLCO-H₂O, and 4 µL sample (1:50 diluted), HPLC-H₂O control, or –RT control. Samples were run in technical triplicates with negative controls for every sample and primer pair. –RT controls were run with the housekeeping gene Actin. qPCR was performed on a Real-Time PCR Cycler (Applied Biosystems, StepOne™Plus Real-Time PCR system, Germany). The PCR conditions were: 95 °C for 20 sec followed by 40 cycles of 95 °C for 3 sec and a final step with 60 °C for 30 sec. In the followed melting program to detect the melting point of the PCR products, the temperature was slowly increased from 65 °C to 90 °C.

2.5.5 qRT-PCR data analysis

Before the data analysis was conducted, raw data were checked with the to the Real-Time PCR cycler associated StepOnePlus software (Applied Biosystems, StepOne™Plus Real-Time PCR system, Germany). The C_T threshold was adjusted 0.2 and meltcurves were checked to exclude non-specific priming. qRT data were analysed with $\Delta C_T = C_T \text{ target gene} - C_T \text{ housekeeping gene}$. Only Actin was used as housekeeping gene for the analysis as there were many missing values in α -Tubulin. Normally, standard deviations between triplicates on differences up to 0.3 between plates are accepted, but they were far too high in this analysis. Tests where triplicates were done on one plate resulted in low standard deviations. I could not figure out where the problem originated. All samples with standard deviations higher than 2.5 between triplicates were excluded from the analysis. High variations were detected for all plates and independent of populations or genes. Therefore, if a signal can be detected, it is assumed that it must be a strong biological signal which is greater than the high “noise” produced here by these high standard deviations. Samples that did not work were not done again due to this high standard deviation. Missing values accounted for ATPc/c': 25%, CAX3: 25%, GPA: 36%, RB: 19%, and SLC4: 19%. All other genes could not been used for the analysis. The results have thus to be taken with constraints.

2.6 Microsatellite analysis

Microsatellites, or short tandem repeats (STR), are demographic markers used to detect patterns of gene flow, migration, and estimation of relatedness on individuals (Oliveira et al. 2006, Schlötterer 2000, Selkoe and Toonen 2006). They are ubiquitous stretches on non-coding sides of the DNA (Schlötterer 2000). By consisting of a repetition motif of one to six bases, they are extremely polymorphic (Li et al. 2002) and have high mutation rates of 10^{-2} to 10^{-6} mutations/ locus/ generation (Schlötterer 2000). These high rates are a result of so-called ‘DNA slippage’ and the efficiency of mismatch repair (Schlötterer 2000). Slip-strand mutations occur when the nascent and template strand realign out of register during DNA replication (Schlötterer 2000). Base-pairing errors occur, which consequently alters the number of repeats on the complementary strand synthesized (Oliveira et al. 2006). These differences can be targeted in a fragment analysis. In a homozygous locus, allele lengths of both homologous chromosomes are the same, whereas in heterozygous loci they are different. Microsatellites can be used to distinguish individuals because of their differentiation on number of repeats on various alleles (Oliveira et al. 2006). For detecting

polymerase chain reaction products of different length, first primers, or oligonucleotides, must be designed. These primers flank the repetitive sites on the microsatellite regions (Schlötterer 2000). In contrast to the highly variable STRs, sequences of the flanking site are generally conserved across individuals (Selkoe and Toonen 2006).

To test for genetic differentiation, a microsatellite analysis was performed with *E. huxleyi* specific primers (Iglesias-Rodriguez et al. 2006, Iglesias-Rodriguez et al. 2002): S15, E9, F08, E10, S37, A08, F11, E5, B12, and E11 (see appendix) for all stock cultures.

2.6.1 DNA sampling and isolation

Cells were filtered on 0.8 µm pore size filter with 25 mm diameter (Whatman, GE Healthcare, UK) with a pressure of 100 mbar. The filter was washed with 500 µL fASW (sterile filtered artificial seawater) and the cell suspension was transferred into Eppendorf® tubes. Tubes were then centrifuged (5424 Centrifuge, Eppendorf, Germany) at 5000 rpm for 10 min. The supernatant was discarded and the pellets stored at -20°C.

DNA isolation was done with an Invisorb Spin Tissue Minikit (250) (Invitex, Germany). Briefly, 400 µL Lysis buffer and 40 µL Proteinase K were added to the cell suspension in a 1.5 mL Eppendorf® tube, incubated at 52 °C under continuous shaking until the lysis was completed, and centrifuged for 2 min at maximum speed. The supernatant was transferred into a new 1.5 mL tube, where 200 µL Binding buffer was added, and it was vortexed for 10 sec. Suspension was transferred onto a spin filter, incubated for 1 min, and centrifuged at 12,000 rpm for 2 min. The procedure was followed by adding 550 µL Wash buffer, centrifuged another min at 12,000 rpm, which was done two times. Finally, the Spin Filter was then placed in a new tube and 200 µL HPLC-H₂O were added, incubated for 3 min, and centrifuged for 2 min at 9,500 rpm to re-bind the DNA from the column.

2.6.2 Microsatellite PCR

Polymerase chain reaction (PCR) was performed with Dream Taq Protocol (Thermo Scientific, Germany, Tab. 3).

Tab. 3: Dream Taq PCR Protocol. Components of per 10 μ L total volume are given.

Buffer 10x	μ L per reaction
dNTPs (10mM each)	1
Primer fwd	0,5
Primer rev	1
Dream Taq Polymerase	1
HPLC H ₂ O	5,9
Template DNA	0,5

Optimal annealing temperatures of primers needed to be determined for enhancing the quality and quantity of the peaks in the fragment analysis (Tab. 4, Tab. 5).

Tab. 4: PCR Protocol. Temperature and time of the single steps during PCR are given. Annealing temperatures used for the individual primers is given in Tab. 5.

	94 °C	3 min	
Denaturation	94°C	1 min	
Annealing	54-60 °C *	1 min	
Extension	72 °C	1 min	27x
	72 °C	10 min	
	4 °C	∞	

Tab. 5: Optimized markers. Optimal annealing temperatures for reaching a good peak quality in the fragment analysis are shown. Results from tests made.

Marker	Optimized Annealing Temperature [°C]
S15	54
E5	57
B12	58
F11	58
E11	59
S37	60
F08	60
E9	60

2.6.3 Fragment analysis

Analysis of the PCR product was performed on an ABI 3130xL genetic analyzer (Applied Biosystems, Germany). Fragment analysis reactions contained 9 μ L of the Master mix (1:36 Rox/ HiDi) and 1 μ L of the post-PCR product, denaturated for 2 min at 95 °C.

2.6.4 Analysis of Microsatellite data

Analysis of raw data was done using GeneMarker version 1.85 (SoftGenetics LLC, United States). Therefore bins and panels were created pairwise with one blue and one green marker. Wright's F_{ST} (1978) was used for population structure assessment. F_{ST} values are ranged between 0, meaning a lack of differentiation, and 1 meaning that compared groups are distinct. In a more fine-scaled division, values of 0.05 for little genetic differentiation, 0.05-0.15 moderate genetic differentiation, 0.15-0.25 great genetic differentiation, and finally >0.25 very great genetic differentiation are separated (Wright 1978). The F-Statistic was done in Arlequin version 3.5 (Excoffier et al. 2005). Plotting of the 3 dimensional principal component plot was computed using GENETIX version 4.05 (Belkhir et al. 2004). The bar diagram was implemented in Structure version 2.3.3, where a Bayesian clustering algorithm detected possible structures among genotypes without any *a priori* assumptions (Pritchard et al. 2000). A genetic admixture model was used and 10000 reiterations of the burn in and 100000 Markov chain Monte Carlo repetitions were performed for cluster from $K=1$ to $K=5$.

2.7 Statistics

Data were analysed to detect potential differences between i) populations over treatments and ii) strains from the same origin using univariate and multivariate analyses of variance (ANOVA and MANOVA) using the software package "R" (R Development Core Team 2005). A one-way ANOVA for single treatments was done as "growth rate/ chlorophyll fluorescence/ size x population" and two-way ANOVAs were first conducted with "treatment x population" to detect overall performance of growth rates, chlorophyll fluorescence, and cell sizes. When they were significant, a Tukey-PostHOC test to determine the strains causing significance was used. To test for homogeneity the Fligner-Killeen test was conducted on significant results. Data were transformed when the test was significant, which is indicated in this case. Normality was tested via Shapiro-Wilk's W- test and graphically examined with a histogram (histograms shown in the appendix). Correlations were done for assessing relationships of growth rates vs. chlorophyll fluorescence, growth rates vs. size, and size vs. chlorophyll fluorescence. Furthermore, Nested ANOVAs were conducted in JMP version 7 (JMP 2007) to find out about variations in strains, performed as "strain [population]" which can be read as "the levels of 'strain' depend on 'population'". For the gene expression analysis, a MANOVA was conducted although having missing values. With the MANOVA tests for interactions of

“treatment and population” were done. Then, a one-way ANOVA for each gene in single treatments was conducted. Correlations were done for assessing relationships of growth rates vs. chlorophyll fluorescence, and growth rates vs. size. Reaction norms were done for testing the interaction of “temperature x strain” of each population, for RT-qPCR data per population for each gene.

3. Results

In this study, differences in physiological responses to warm and cold temperatures in strains from a northern and a southern *Emiliania huxleyi* population were detected. Population structure and morphotypes of all individual strains were determined. Physiological responses included growth rates μ , sizes, effective quantum yields, and gene expression as indicator for the 'molecular phenotype'. These responses were first investigated on the population level, and later on a strain level, and possible relationships between measured parameters were correlated. Lastly, reaction norms were conducted to detect genotype-by-environment interactions.

3.1 Population characteristics

3.1.1 Population structure

In the microsatellite analysis, pairwise comparison showed population differentiation with an F_{ST} of 0.148 ($p < 0.01$), which was graphically presented in Fig. 8. The principal component analysis (PCA) plot is showing genetic diversity as distance, based on data for five microsatellite primers. Individuals represented as dots in the plot, from same locations were grouped together and therefore showed genetic separation. The variance (thus the distance between the dots) was higher within the Azores' than the Bergens' genotypes.

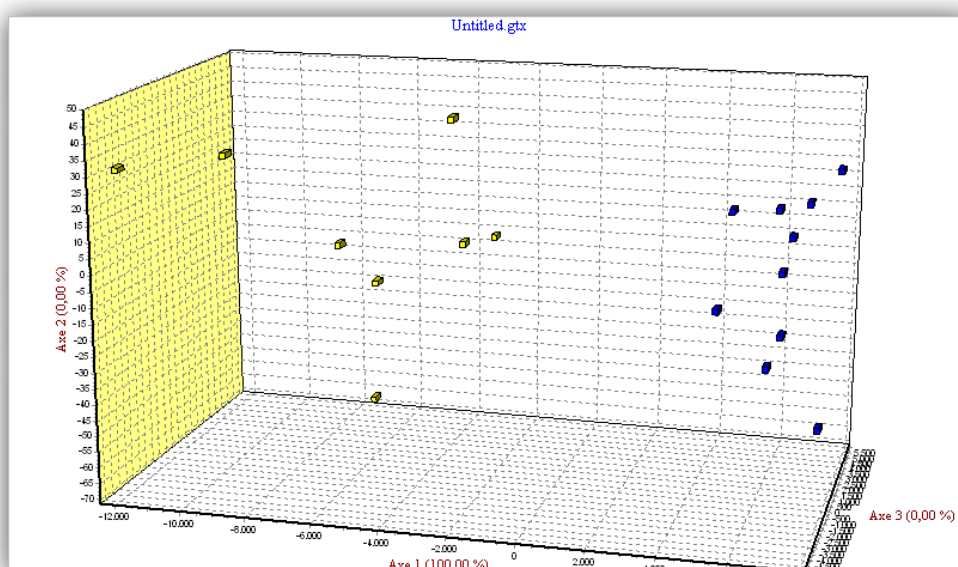


Fig. 8 Genetic diversity as distance. Each dot represents one individual. yellow= Azores, blue= Bergen. The plot is based on data for five microsatellite markers. Two groups can be observed.

The bar diagram (Fig. 9) illustrates all individuals from both locations and gives their discrimination whether they are more similar to one or the other population. A red bar represents the likelihood of a genotype to be clustered within the Bergen group, whereas a green bar indicates the likelihood to be clustered into the Azores group. The most likely number of genetic clusters was $K=2$, thus two distinct groups could be detected. Strain M17 from the Azores group was arranged closer into the Bergen group. Further, two of the ten strains from the Azores were found to have identical alleles in all microsatellite markers used for analysis. Only one of these strains was used in the experiment. Also B1/75 was used in this analysis and alleles could be detected. As microsatellite primers are supposed to be *E. huxleyi*-specific, there must be *E. huxleyi* cells in the stock culture.

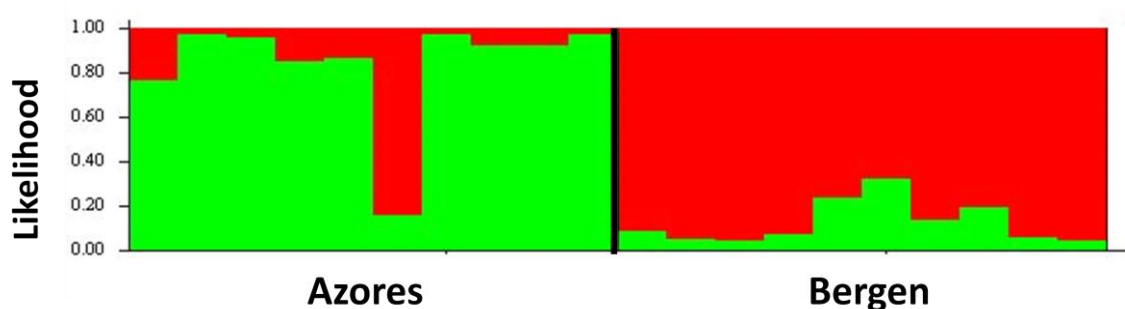


Fig. 9 Bar diagram of Bayesian clustering. Each bar represents the likelihood of one individual to be clustered rather to the one or the other group. From left to right. Azores: A1/M23, M16, A2/M22, A3/M21, A4/M19, M17, A5/M13, A6/M10, M8, M7. Bergen: 96, B2/62, 73, 51, 42, B4/85, B1/75, B5/63, B3/41, B6/17. $K=2$, grouping into two populations. Assignment of individuals into groups based on similarity.

From the ten microsatellite markers, only five could be used in this analysis. Marker E10 had to be excluded because there were no signals in all samples, while the markers F08, E5, and E11 showed too many missing alleles for an analysis. Marker A08 worked for the Bergen strains, but failed in the PCR of the strains deriving from the Azores.

3.1.2 Morphotypes

SEM-images revealed that all strains from both sites, except stain B1/75, were of morphotype A. Lith sizes (sizes of the scales) were about 3-4 μm , and they had robust distal shields. The strains from Bergen, Norway (Fig. 10) had a thick inner tube, and the central area was calcified consisting of a thin plate. In the cultures of B1/75, most cells had no coccoliths, but there were still some coccospheres and single coccoliths found in the sample. It could not be distinguished whether this was a different organism or a non-calcifying *E. huxleyi* strain therefore it was excluded from the analysis of the experiment.

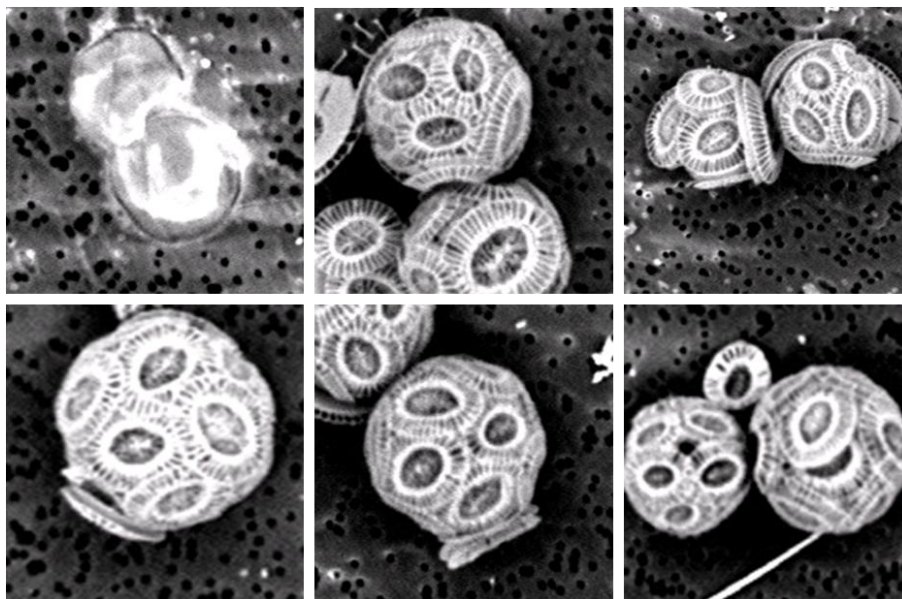


Fig. 10: SEM-images of Bergen. Left to right. Top: B1/ 75, B2/ 62, B3/ 41, Bottom: B4/ 85, B5/ 63, B6/ 17. Cells of strain B1/75 were widely not having coccoliths therefore it was excluded from the analysis.

Fig. 11 is showing all strains from the Azores having coccospheres. In comparison to the isolates from Bergen, inner tubes were thinner, and the central area thicker.

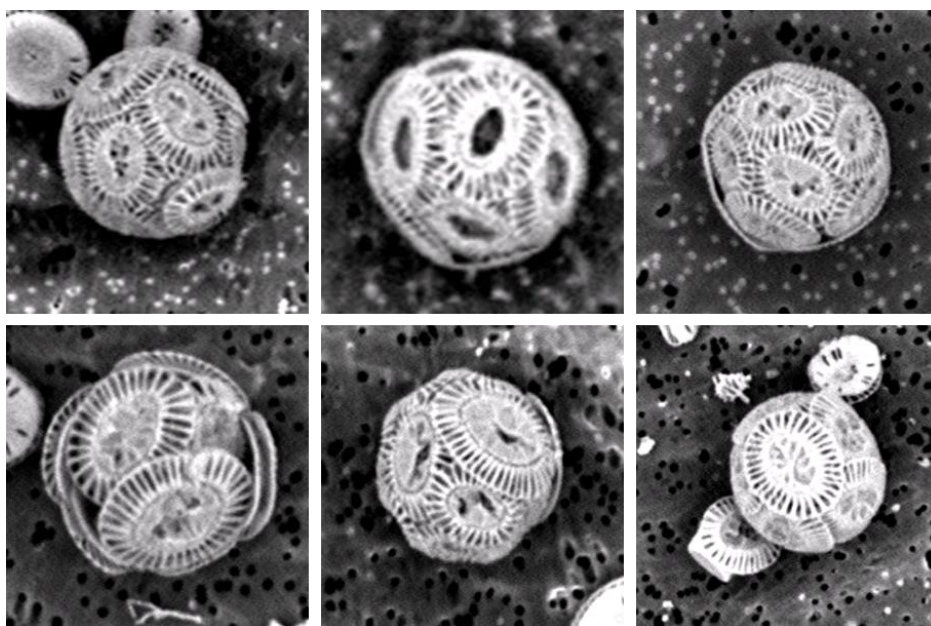


Fig. 11: SEM-images of Azores. Left to right top: A1/ M23, A2/ M22, A3/ M21, bottom: A4/ M19, A5/ M13, A6/ M10

3.2 Population comparison

3.2.1 Growth rates of populations

Differences between temperatures and populations were detected in the growth rate measurements. Two-way analysis of variance detected a population effect ($F=81.952$, p

<0.0001), a temperature effect ($F=10777.954$, $p < 0.0001$), and an effect in the interaction of these two ($F= 45.282$, $p < 0.0001$, data were cube-transformed). Mean growth rate in the cold temperature was $0.479 \pm 0.117 \text{ d}^{-1}$, and in the warm $1.557 \pm 0.017 \text{ d}^{-1}$ (Fig. 12). The range in the 8°C treatment was from minimum 0.382 to max 0.595 d^{-1} , while in the warm temperature treatment growth rates $[\mu]$ reached values from 0.446 to 0.649 d^{-1} among strain means.

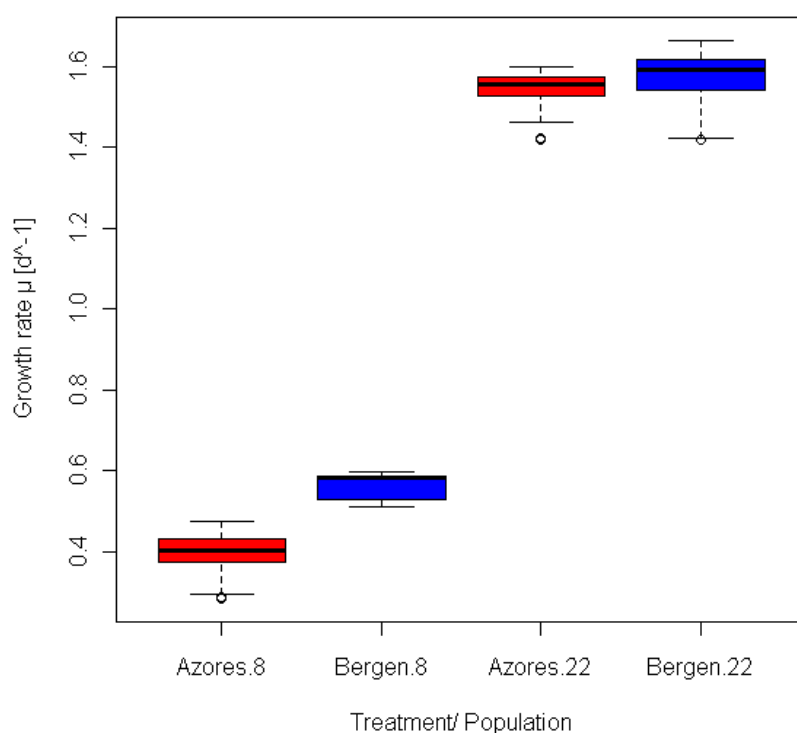


Fig. 12: Mean growth rates μ of populations. Growth rates of populations in both treatments.

In the cold treatment, Bergen strains grew faster with a mean of $\mu = 0.561 \pm 0.036 \text{ d}^{-1}$, in comparison to Azores strains with $\mu = 0.396 \pm 0.063 \text{ d}^{-1}$ (one-way ANOVA, $F=217.88$ and $p < 2.2e-16$). Cultures from the Azores had to be counted and sampled two days later in order to get reliable counts and sufficient amounts of RNA for gene expression. In the warm treatment both populations grew approximately in the same speed with growth rates of $\mu = 1.159 \pm 0.077 \text{ d}^{-1}$ in Bergen strains and $1.545 \pm 0.04 \text{ d}^{-1}$ in Azores strains (one-way ANOVA, $F= 2.243$, $p= 0.14$).

3.2.2 Chlorophyll fluorescence

The pulse-amplitude modulated fluorometry measurements showed a similar pattern to the growth rates. Significant differences could again be detected among populations ($F= 11.534$, $p= 0.0009627$), treatments ($F= 103.783$, $p < 2.2e-16$), and their interaction ($F= 22.194$, $p= 7.514e-06$, data were cube-transformed) in the multivariate ANOVA. Maximum effective quantum yields (Φ_{PSII}) had a mean of 0.532 ± 0.028 at 8°C , and were higher in 22°C with 0.592 ± 0.006 (Fig 13).

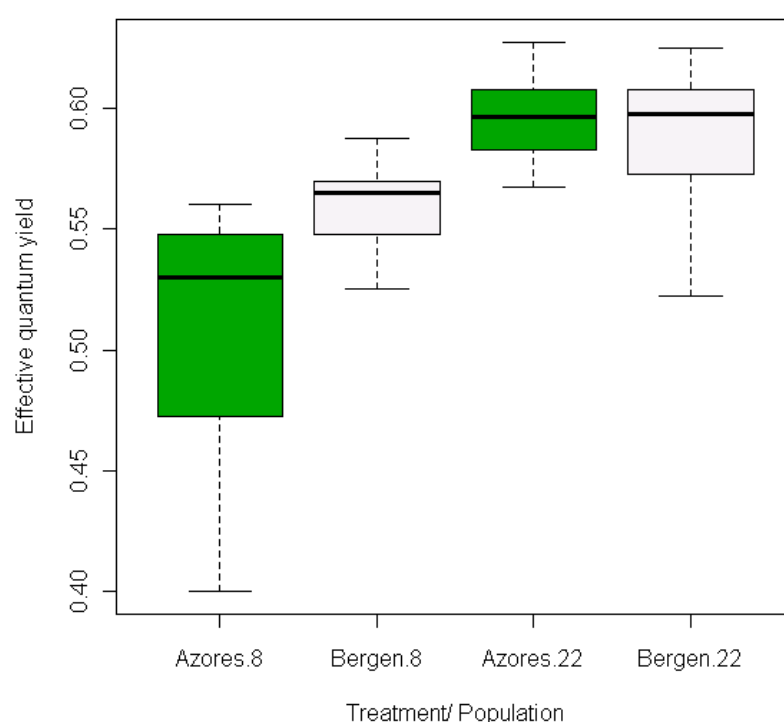


Fig. 13. Mean effective quantum yield of PSII of populations. Effective quantum yields of both populations measured in warm and cold treatments, at culture conditions.

In the cold treatment, mean quantum efficiency yields were lower in the Azores group with 0.523 ± 0.047 than in the Bergen 0.553 ± 0.025 (one-way ANOVA, $F= 22.692$, $p= 1.517e-05$). Effective quantum yields were same at the high temperature with 0.587 ± 0.025 in the Bergen group, and 0.596 ± 0.154 in the Azores group ($F= 1.5665$, $p= 0.2162$).

3.2.3 Growth-Chlorophyll fluorescence-Size relationships

As similar patterns were observed in the growth rates and pulse-amplitude modulated fluorometry, this lead to the question whether relationships between parameters could be observed. Therefore, measured responses were correlated to each other.

First, regressions were made for growth rates vs. maximum quantum efficiency yields (Fig. 14). In the 8°C treatment, a high correlation was obtained with an R^2 of 0.632 ($p < 0.0001$) and a slope $m = 0.3554$. When splitting the regressions into single population fits, it was found that R^2 is higher in the Azores with $R^2 = 0.6691$ ($p < 0.0001$), while the fit in Bergen is a bit lower with $R^2 = 0.5805$ ($p < 0.0001$). However, the obtained correlation in the cold treatment was not found in the warm regime. With a fit of $R^2 = 0.0368$ ($p = 0.142$), the correlation was weak. This lack of fit is not caused by one population, R^2 was low in both treated groups (Bergen $R^2 = 0.0846$, $p = 0.119$, Azores $R^2 = 0.0067$, $p = 0.668$).

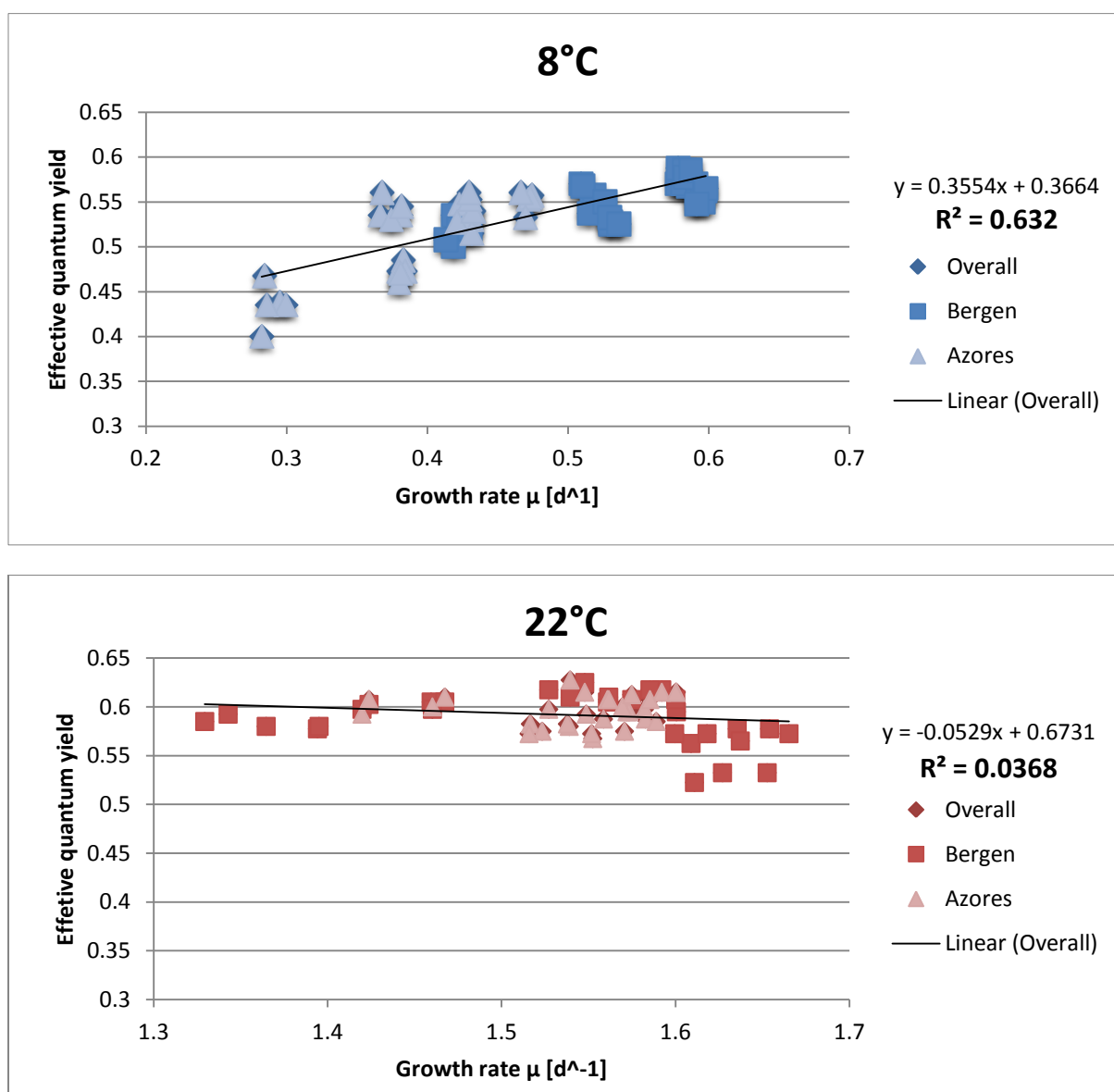


Fig. 14: Correlation between growth rate [μ] and $\Phi PS II$ at treatment temperatures of both populations. Top: Correlation for 8°C, Bottom: Correlation for 22°C. Different symbols are showing the populations. Slope and coefficient of determination R^2 are given in the top right of the graphs.

A linear relationship was found in the growth rate-size relationship ($R^2 = 0.9384$, $F = 1644.072$, $p < 0.0001$). There was a negative correlation between growth and size from cold to warm treatments with a slope of $m = -1.3827$. The coefficient of determination was a bit higher in the Azores with $R^2 = 0.982$ ($p < 0.0001$), than Bergen $R^2 = 0.9586$ ($p < 0.0001$). A correlation was also found when plotting the responses of populations in different treatments against growth rate μ and size, showing that Azores were bigger in both treatments.

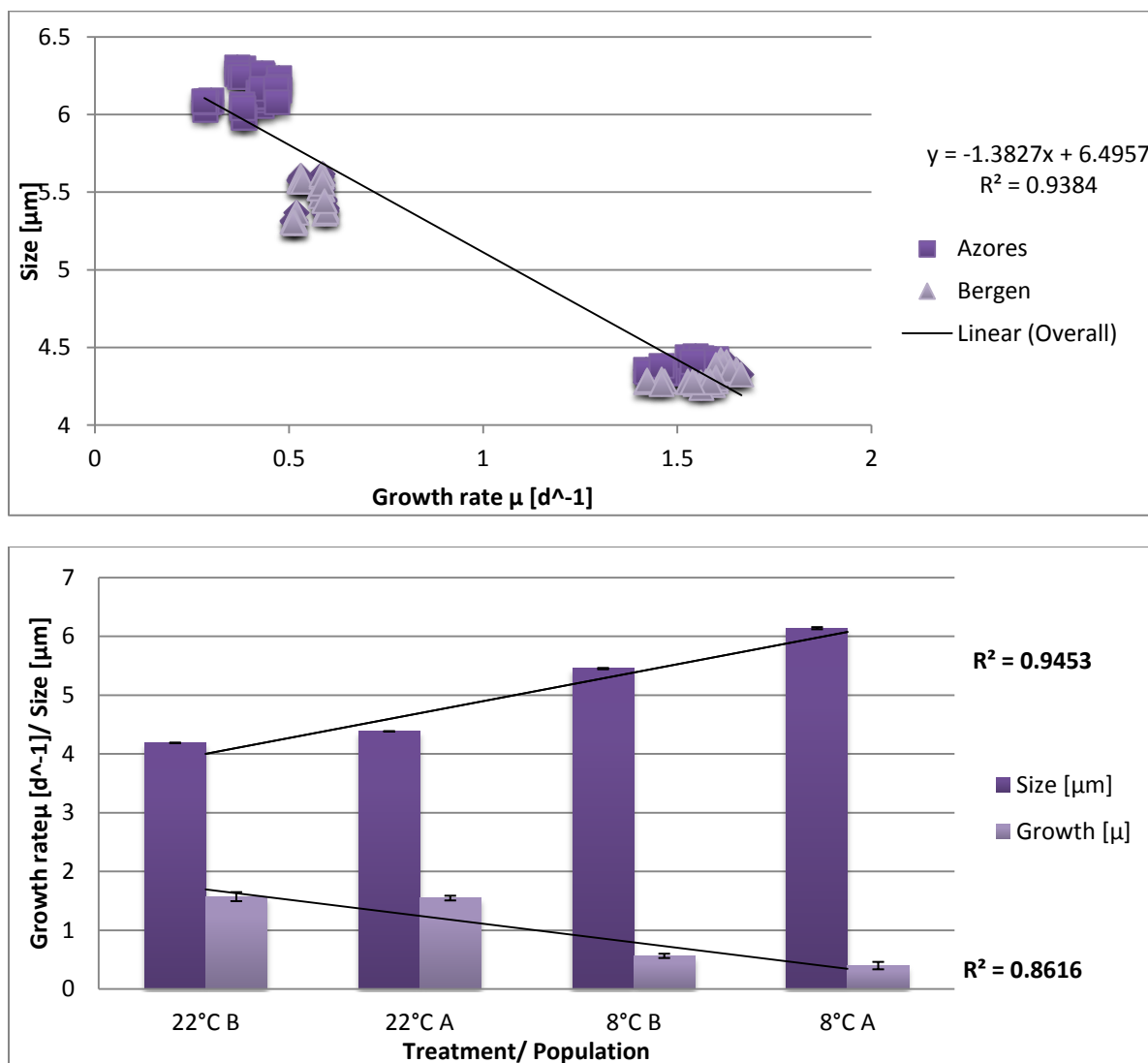


Fig. 15: Relationships between Growth/Size and Temperature. Top: Correlation growth rates and size. Bottom: Mean size and growth rate of Populations in both treatments. Slope and coefficient of determination R^2 are given in the top right of the graphs.

3.2.4 Gene Expression

Of the tested candidate genes, only Actin, GPA, CAX3, SLC4, and RB could be used for analysis. In the standard curves, R^2 or efficiencies were not in the requested range in all other primers. Primers for Hsp 70 did not work at all, Hsp 90 (both Kaufman 2007) showed a weird signal in the $-RT$ control (see appendix). A product was amplified in high amounts

much earlier than signals of normal cDNA standard curve concentrations. I found the same signal for CaM (Richier et al. 2009). I tested this twice with different –RT controls but found the same results.

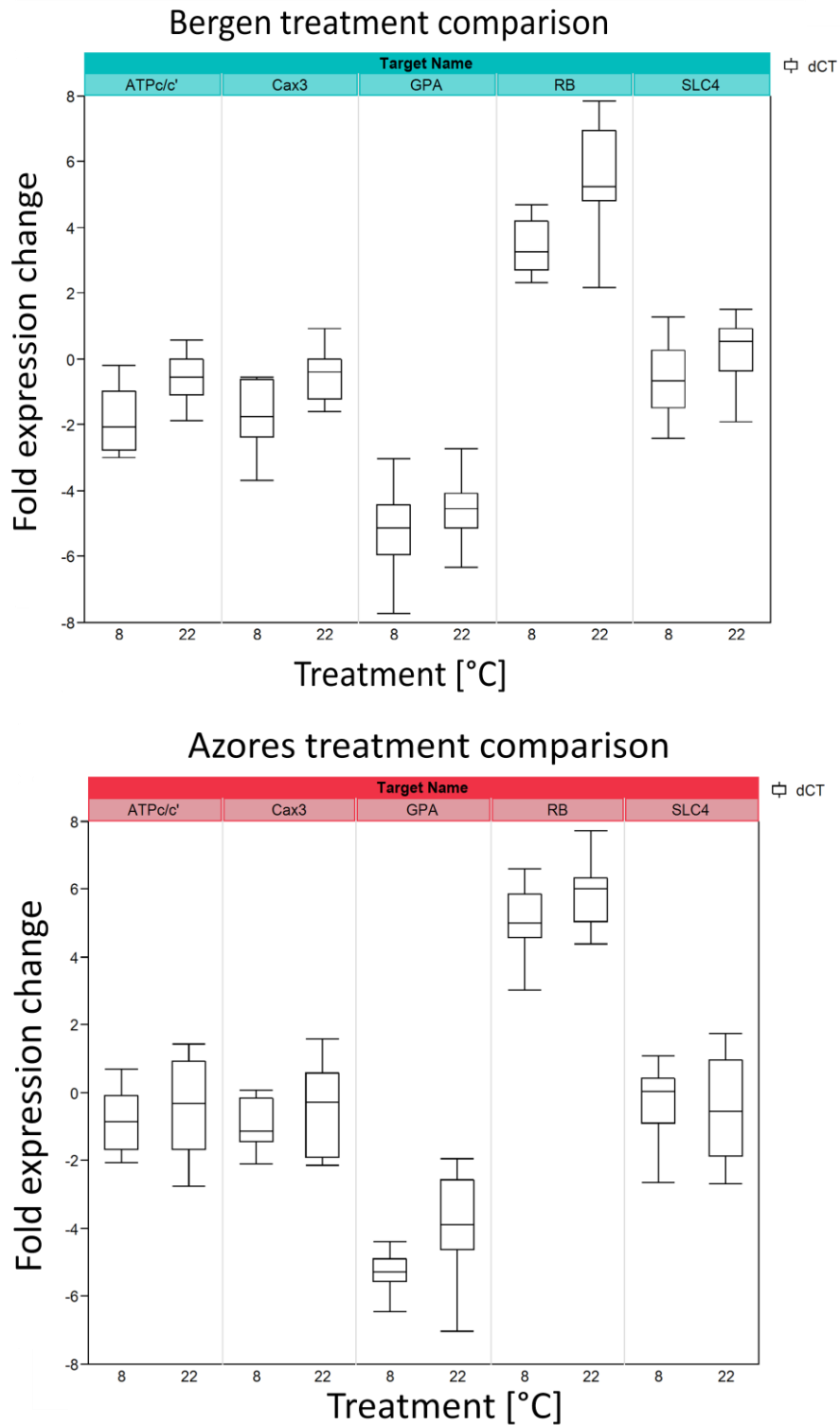


Fig. 16: Treatment comparison of Gene expression. Top: Comparison of Bergen population at 8°C and 22°C, Bottom: Azores population at 8°C and 22°C. Y-axis: dCT gives the fold expression change in comparison to the housekeeping gene.

Genes were in general more up-regulated in the warm treatment, where the difference was more striking in the Bergen group (Fig. 16). Treatment effects were found in CAX3 (two-way ANOVA, $F = 5.5114$, $p = 0.0022$, treatment: $p < 0.0003$), GPA (3.871 , $p = 0.0149$, treatment: $p = 0.0035$), and RB ($F = 12.445$, $p < 0.0001$, treatment: $p < 0.0001$).

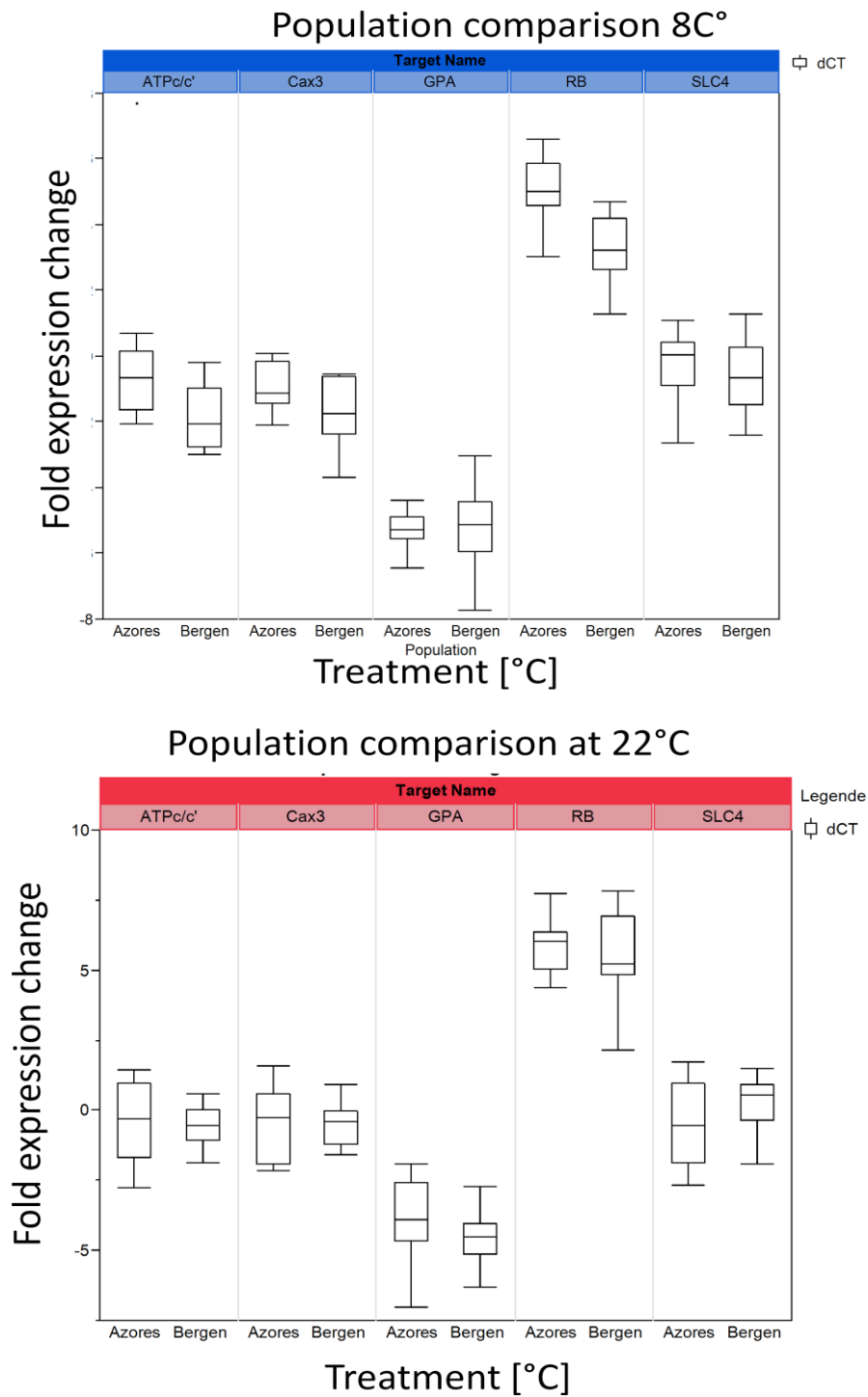


Fig. 17: Population comparison of Gene expression. Left: Comparison of populations in 8°C, right: Comparison of populations in 22°C. Y-axis: dCT gives the fold expression change in comparison to the housekeeping gene.

Fig. 17 is showing a population comparison in the different treatments. The overlap was high, population differences were seen only in RB (two-way ANOVA, $F= 12.445$, $p < 0.0001$, population: 0.0003), where the expression was higher in the Azores group at 8°C and at 22°C. The only population x treatment effect was found in RB, seen in a higher regulation within the Azores group at 8°C.

Tab. 6: Nested ANOVA Gene expression. Strain[Population] can be read as 'the levels of strain depend on population'. Significant results $p= 0.05$ are written in bold letters. Df= degrees of freedom.

		Df	ATPc/c'	CAX3	GPA	RB	SLC4
8°C	Strain[Population]	6	0.1488	< 0.0001	0.0284	0.2317	0.0005
	Population	1	0.063	0.0024	0.9571	0.0001	0.8875
22°C	Strain[Population]	6	0.0071	0.168	0.2614	0.0334	< 0.0001
	Population	1	0.694	0.8154	0.1216	0.3008	0.0036

To investigate whether the variation between or within populations was higher, a Nested ANOVA was conducted. In the 8°C treatment, population differences were found in CAX3 and RB, being more expressed in the Azores group (Fig. 17). In the warm treatment only in SLC4 was a difference, as being at average higher expressed in the Bergen group. Differences between were detected at low temperature in CAX3, GPA, and SLC4, in high temperature in ATPc/c', CAX3, RB, and SLC4 (Tab. 6).

3.3 Genotype variation and interaction

Inter-strain variation was generally high between strains, independent of its origin. First, physiological measurements were analyzed at the strain level. In the second part, linear reaction norms on growth and gene expression were performed. There, the overall plasticity between the two populations was compared, followed by detailed analysis of single genotypes of both origins. Lastly, reaction norms of the populations in warm and cold temperature were analyzed for each gene.

3.3.1 Growth rates of strains

Nested ANOVA tested whether differences came from population effects or whether this was due to strain variation. In the cold treatment, effects were found in populations ($F= 861.307$, $p < 2.2e-16$), in strains ($F= 148.216$, $p < 2.2e-16$), and in their interaction ($F= 10.299$, $p= 0.002303$). The boxplot of strains from both locations (Fig. 18) depicts the high variation as there is almost no overlap of the boxplots, nearly all strains had a different growth rate. A

weird increase with strain number is shown in Fig. 18. Because strains were not counted one after the other by increasing strains number, a time effect can be excluded.

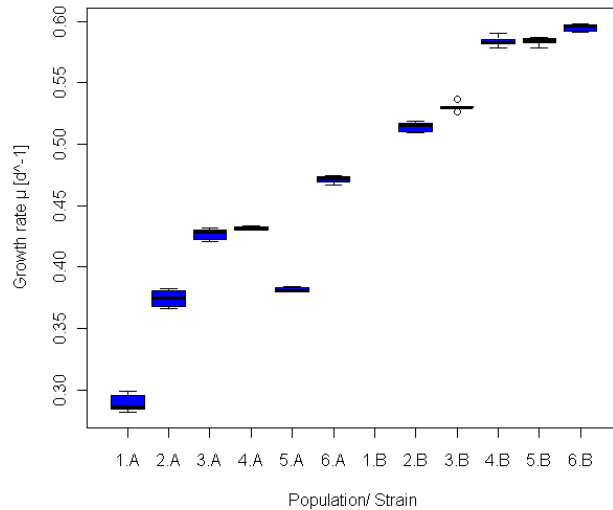


Fig. 18: Growth rates in strains at 8°C. Individual strains from both locations in the cold treatment as boxplots. As strains were not counted in the order as shown there, the increase in growth rate and cell number cannot be due to a time effect.

At 22°C, nested ANOVA gave no population effect ($F= 2.6657$, $p= 0.10870$), only a slight strain effect ($F= 5.5902$, $p= 0.02191$), as well as a slight interaction effect ($F= 6.3986$, $p= 0.01455$). As depicted in Fig. 19, mean growth rates of strains were similar, only strains M13 (A5) and B63 (B5) grew slower.

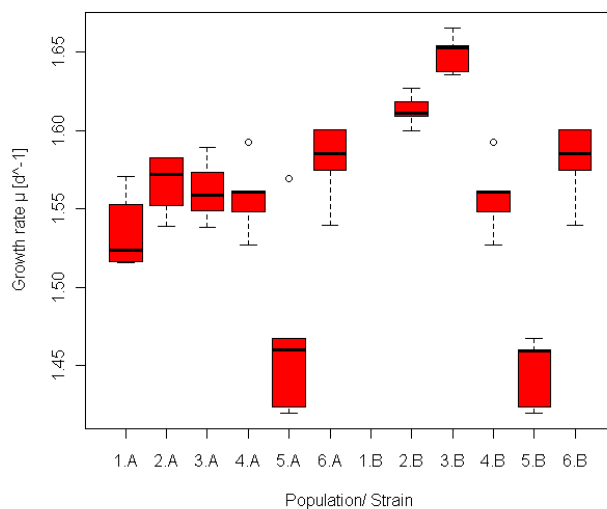


Fig. 19: Growth rates in strains at 22°C. Individual strains from both locations in the warm treatment as boxplots.

3.3.2 Photosynthetic efficiency of PSII in single strains

There was a population ($F= 26.2357$, $p= 4.671e-06$), and strain effect ($F= 9.2871$, $p= 0.003651$) in the cold treatment chlorophyll fluorescence measurements at 8°C. It can be seen that high variation derived from responses of single strains, where maximum quantum efficiency of strains A1/ M23 and A5/ M13 were lower in comparison to the other strains (Fig. 20).

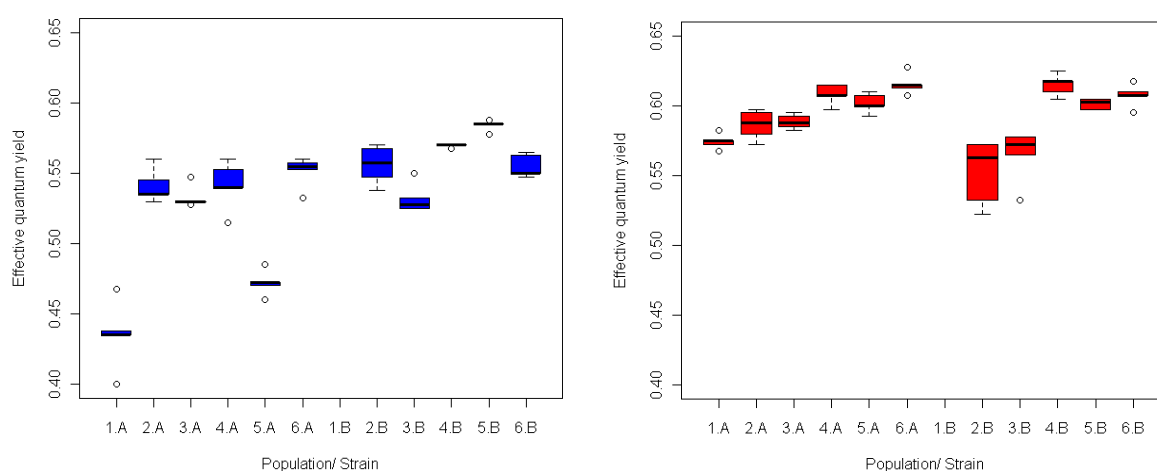


Fig. 20: Effective quantum yield of PSII in single strains. Left: Individual strains from both locations at 8°C, right: Individual strains from both locations as 22°C.

In the 22°C treatment of PAM fluorometry measurements, a strain effect ($F= 68.5977$, $p= 5.272e-11$), and a population* strain effect $F= 7.1594$, $P= 0.01$), but no population effect ($F= 3.7466$, $p= 0.05847$) were seen. Variation of the replicates B2/ 62 was high within this strain (Fig. 20).

3.4 Reaction norms of growth

Reaction norms give genotype-specific environment-phenotype functions showing how a genotype's phenotype changes with changing environmental conditions. They can be determined with a graph, where each line represents the responses of a genotype. The slopes show plasticity of genotypes. When different slopes are presented, this indicates a genotype-by-environment interaction of a population or a single genotype, and further detectable by ANOVA. Reaction norms were conducted to test for population x environment interactions for the mean performance of populations, and genotype x environment interactions were tested to compare the performance of single strains within a population.

3.4.1 Reaction norms over population

In a population comparison of plasticity, the regression of Azores was steeper with $m=0.0821$ to the Bergen with $m=0.072$ (Fig. 21), showing a higher plasticity of the Azores population (multivariate analysis of variance, $F=690.308$ and $p<0.0001$). All single parameters and the interaction of temperature and population were significant (temperature: $F=2004.897$, $p<0.001$, population: $F=15.56$, $p=0.0009$, temperature*population: $F=8.5992$, $p=0.0089$).

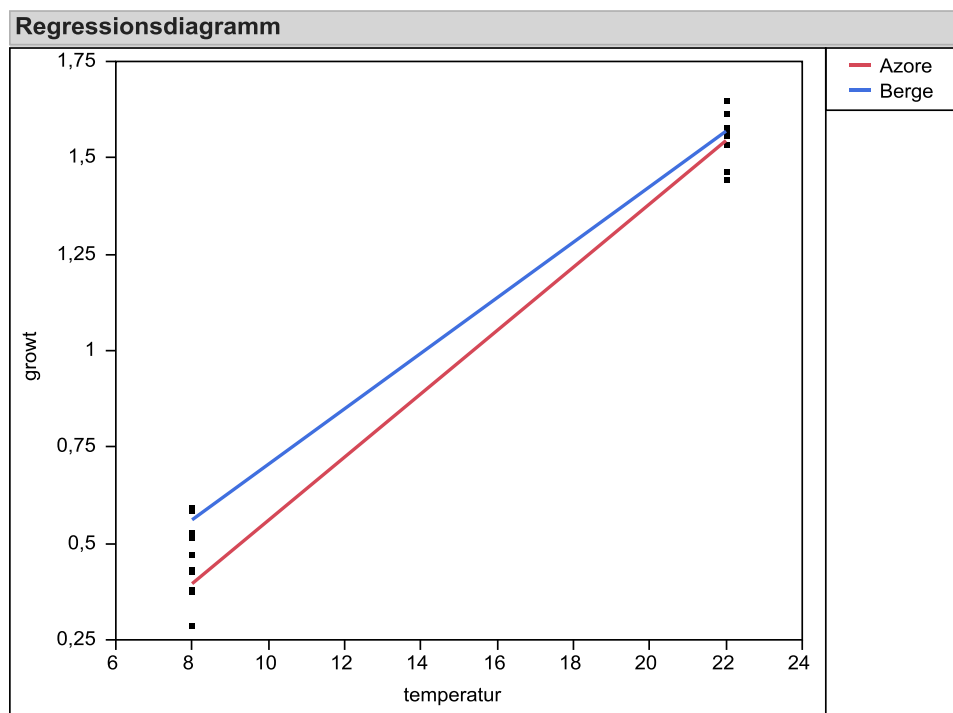


Fig. 21: Reaction norm of populations over both temperatures. Mean growth rates μ over both treatments. X-axis: Temperature in °C, y-axis: growth rate μ [per day]. Red: Azores, blue: Bergen.

3.4.2 Reaction norms over strains

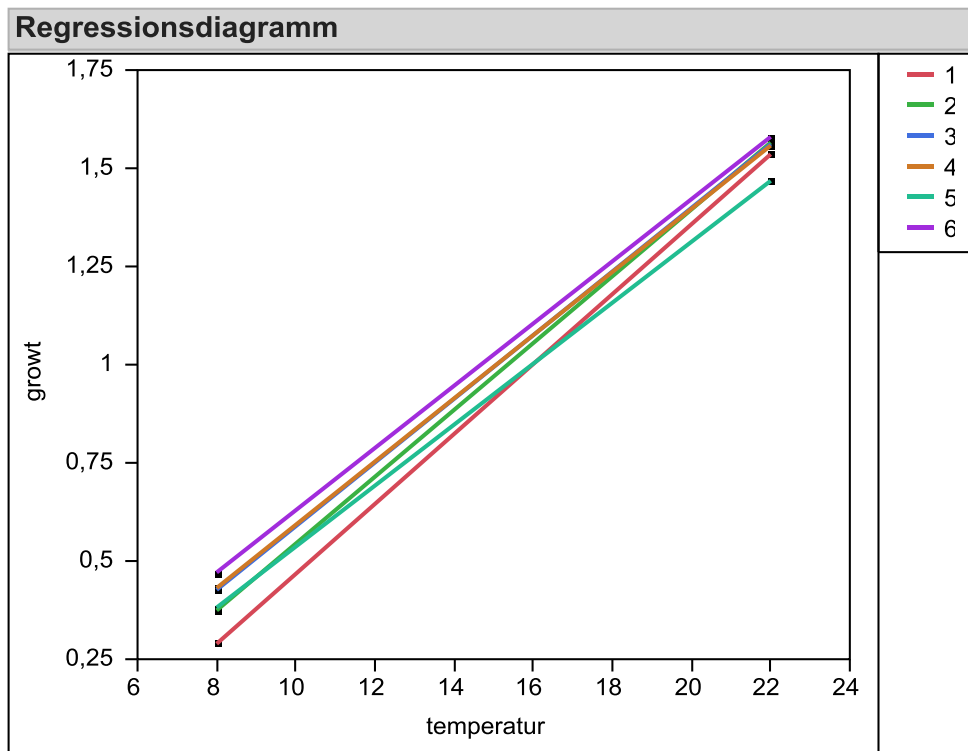


Fig. 22: Reaction norms of genotypes in Azores group. X-axis: Temperature in °C, y-axis: growth rate μ [per day]. Each slope represents the response of one strain over both treatments.

Genotype-by-environment interactions were found in the Azores group ($F= 3407.66$, $p < 0.0001$). These effects could be seen in an effect in temperature ($F= 37211.53$, $p < 0.0001$), strain ($F= 36.118$, $p < 0.0001$) and the interaction of the two parameters ($F= 16,433$, $p = < 0.0001$). The plasticity of strains A1/ M23 and A2/ M22 were of highest change in comparison to other strains (Fig. 22). A6/ M10 and A4/ M19 reacted similar to the different temperatures, as their slopes were relatively parallel. Additionally, A6/ M10 performed best in both temperatures. A5/ M13 on the other hand showed the smallest reaction.

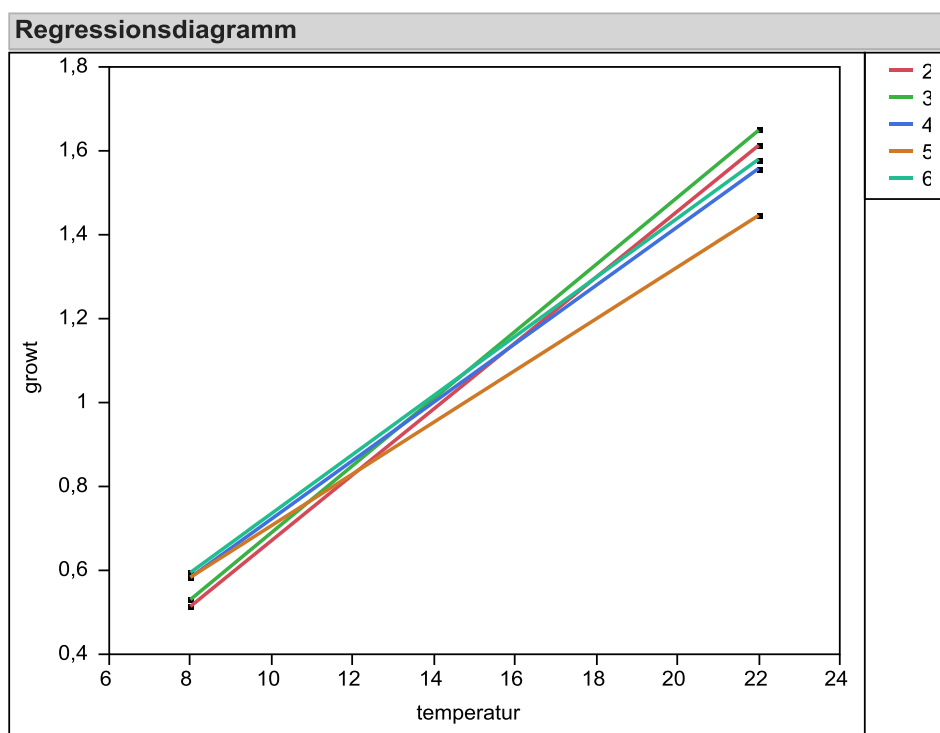


Fig. 23: Reaction norms of genotypes in Bergen group. X-axis: Temperature in °C, y-axis: growth rate μ [per day]. Each slope represents the response of one strain over both treatments.

In the Bergen population, reaction norms were as heterogeneous as the Azores strains ($F=7014.13$, $p < 0.0001$). Effects in temperature ($F=62415.22$, $p < 0.0001$), strain ($F=44.949$, $p < 0.0001$), and the interaction temperature* strain ($F=133.04$, $p < 0.0001$) were detected. There was no genotype performing best in both treatments (Fig. 23). Namely strains B2/ 62 and B3/ 41 showed a high plasticity. Strains B4/ 85 and B6/ 17 had similar reaction slopes. Last, strain B5/ 63 showed the lowest plasticity.

3.4.3 Reaction norms of Gene expression

Genotype-by-environment interactions were also detected in the gene expression. Reaction norms were either significant between treatments, strains, or both (Tab. 7). Only in GPA, there were no significant differences. Detailed linear reaction norms are shown in the Appendix. Treatment effects in the Bergen population for all genes analyzed except GPA, while in the Azores group only in GPA and RB. Strain effects were found in four genes (ATPc/c', CAX3, GPA, SLC4) in the Azores group and in three in the Bergen group (CAX3, RB, SLC4). There were treatment x strain effects in ATPc/c' and GPA expression in the Azores group, and CAX3 and RB in the Bergen group.

Tab. 7: ANOVA Genotype-by-environment interactions of gene expression. Treatment (Environment) as fixed and strain (Genotype) as random factors, given for each gene. Significance level $p=0.05$.

		Azores		Bergen	
		F	p	F	p
ATPc/c'	treat	1.2117	0.2819	15.8611	0.0008
	strain	5.8182	0.0039	1.8993	0.1640
	treat*strain	3.6061	0.0279	1.5415	0.2413
CAX3	treat	2.7905	0.1068	16.445	0.0007
	strain	12.029	<0.001	3.4932	0.0359
	treat*strain	1.8158	0.1690	5.0751	0.0095
GPA	treat	8.4176	0.0099	3.5889	0.0734
	strain	9.6289	0.0006	1.5489	0.2363
	treat*strain	12.9481	0.0001	3.1061	0.0525
RB	treat	6.1936	0.0198	20.0295	0.0002
	strain	1.5920	0.2163	4.0260	0.0188
	treat*strain	1.0593	0.3840	3.4874	0.0313
SLC4	treat	0.5588	0.4617	5.3743	0.0293
	strain	26.2354	<0.001	4.7553	0.0097
	treat*strain	1.6960	0.1934	2.7369	0.0657

4. Discussion

Local adaptation occurs when populations in different environmental conditions evolve traits that are advantageous in these habitats (Kawecki and Ebert 2004). Reciprocal transplant experiments can test for local adaptation using the assumption that at each geographic site the native population has a higher fitness than any other population of the same species (Savolainen 2011). Genetic differentiation of two geographically distinct populations was investigated using microsatellite markers. Moreover, reciprocal growth experiments were used to resolve patterns of adaptation and the role of phenotypic plasticity in the globally distributed phytoplankton species *Emiliana huxleyi*. Within this study, such a reciprocal experiment was conducted in which strains isolated from two different geographic origins were grown in their own native temperature and in the temperature of the other location. Two questions concerning evolutionary processes of *E. huxleyi* were addressed. First, the difference in population specific temperature response should be assessed. Different population structure and physiological responses give hints on ecotype speciation and are a hint for local adaptation. By amplifying microsatellite loci from field isolates and determining their maximum growth rates, genetically and physiologically distinct populations of a diatom were found to exist in two adjacent estuaries (Rynearson and Armbrust 2004). Here I used a similar approach, although the strains derived from geographically widely separated origins. Second, phenotypic plasticity under two temperatures was assessed for each strain and over the populations. The magnitude of strain specific plasticity was investigated by comparing the performance of strains in different temperatures. Reaction norms were analyzed to retrieve possible genotype-by-environment interactions.

4.1 Population structure and characteristics

Microsatellites were used to assess the population structure of the strains from Bergen and the Azores. Population structure analysis revealed a moderate to strong genetic variation with an F_{ST} of 0.148 ($p < 0.01$) according to Wright (1978). This was in concordance to findings of Iglesias-Rodriguez et al. (2006). By analyzing 85 strains of *E. huxleyi* from different ocean regions, they found a $F_{ST} = 0.09894$; $p < 0.05$. Here, we used the same primers of which some primers were not working and primer A08 worked in the Bergen strains, but not in the

Azores strains. This could be explained by null alleles that occur when sites where primers attach have many point mutations, so that primers cannot bind to the DNA and might already be an indication for genetic divergence. Based on microsatellite analysis, two populations were detected according to the geographical origin of the strains. As illustrated in Fig. 8, the Bergen population showed lower variability as the distances of each individual were closer than in the Azores group. Groupings into two different populations presented in the bar diagram (Fig. 9), lead to an interesting finding of one southern strain (M17) being rather grouped into the northern population. A possible explanation could be based on the location of the origin of strains: While Bergen strains come from a rather isolated fjord, the Azores strains were isolated at a site in the open North Atlantic. The likelihood that cells from the Bergen area were drifted to the Azores may be much higher than the other way round. Unexpectedly, I found two strains being identical in all alleles, whereas in the study by Iglesias-Rodriguez et al. (2006) isolates from a coastal fjord sampled from the same water body were found to be genetically distinct in microsatellite alleles. Maybe in identical isolates were too few primers used to detect genetic separation or isolates were spreading within the bloom. Alternatively, there may have been a cross-contamination in culturing work before I got the strains. Nevertheless, limitation to gene flow as found here is a prerequisite for local adaptation (Kawecki and Ebert 2004). Also Iglesias-Rodriguez et al. (2006) suggested that a moderate genetic differentiation may indicate selection of different strains due to environmental conditions or barriers by current systems. A study comparing the diatom *Ditylum brightwelli* in two estuaries found genetically distinct populations using microsatellite markers, as well as maximum growth rates between the isolates to be different, which indicated different physiological capabilities (Ryner and Armbrust 2004). They found genetic and physiological differentiation between populations from intermixing estuaries and concluded a restriction in genetic exchange through differential selection. A study on the diatom *Pseudo-nitzschia pungens* revealed strain isolation by distance patterns contrasting to Ryner and Armstrong (2004), and additional phylogeny analysis supported the idea that population structuring may have led to speciation which is important for diversification in marine phytoplankton (Casteleyn et al. 2010). Concordantly with these studies, I found genetic differentiation of the Bergen and the Azores populations. This may be explained by limited gene flow, differential selection at the two locations or most likely a combination of both. Altogether, these findings support the idea that

biogeography also exists in the microbial world, which is in contrast to the hypothesis 'everything-is-everywhere' which suggests that dispersal of microbial species is potentially ubiquitous due to only rarely restriction by geographic barriers (Finlay 2002, Finlay and Clarke 1999).

Scanning electron microscopy (SEM) images revealed that all strains except of one could be identified as morphotype A. This morphotype was also found to be dominant in North East Atlantic *E. huxleyi* blooms (van Bleijswijk et al. 1991), and at the Norwegian coast (Young 1994). For comparison, it is important that all strains belong to the same morphotype. This is because different morphotypes were shown to be genetically different (Medlin et al. 1996), and are distinct in several phenotypic characteristics, e.g. growth (Paasche and Klaveness 1970).

4.2 Between-population differentiation

To investigate between population differences, exponential growth rate (μ) as fitness proxy, effective quantum yield of PSII (Φ_{PSII}) as indicator for photosynthetic efficiency of PSII, cell size, and gene expression of candidate genes involved in calcification, proton exchange, and photosynthesis were measured. The hypothesis, that populations perform best at their natural temperature regime could partly be confirmed: At 8°C, Bergen strains grew on average 1.4 times faster than Azores strains, while at 22°C both populations grew approximately equally fast, with a tendency of Bergen strains to be faster. Not surprisingly, growth rates were higher at 22°C because metabolic processes are faster at higher temperatures as long as temperature does not exceed the optimum. As Bergen strains are exposed to low temperatures in their natural environment, they seem to have developed mechanisms that they can deal better in this temperature. Strains from the Azores are probably not confronted to such low temperatures in their home location with average temperature ranges of 15- 25°C (Lafon et al. 2004). The Bergen group, on the other hand, is regularly faced with high temperature fluctuations (Hurrell 1995), in the range of 3-20°C (Surf-forecast.com). In a study comparing six coccolithophorid strains, Buitenhuis et al. (2008) supposed that species inhabiting warm-water habitats are likely to be genetically adjusted to higher temperatures than are those inhabiting temperate regions. Another study found that coastal strains were more tolerant to low salinities than open ocean strains (see Paasche 2001). Similar to these studies, there might also be differences in strains from Bergen being potentially more tolerant to temperature variations according to the higher

annual environmental fluctuations. However, 22°C is still close to the range Bergen strains are naturally encountered to, so this temperature is likely not causing stress to the Bergen strains. In an experiment where these strains were grown at higher temperatures, Azores strains had higher growth rates in comparison to Bergen strains. At 28°C, while Azores strains were still growing, strains from Bergen could grow not anymore (Yong Zhang, personal communication).

Effective quantum yields of PS II (Φ_{PSII}) at culturing conditions of $140 \mu\text{mol m}^{-2}\text{s}^{-1}$ were generally higher in both populations at 22°C than at 8°C. Higher average yields were found for Bergen than for the Azores at 8°C, while there were no significant differences between the populations at 22°C. In a study on two potential ecotypes of the chlorophyte *Valonia utricularis* from a cold-adapted Mediterranean and from a warm-adapted Indian Ocean isolate, it was shown that these isolates have different potentials for acclimation of PSII at suboptimal growth temperatures (Eggert et al. 2003). Another example for photosynthetic responses of marine macrophytes was given in a comparison of two *Laminaria* populations from the western North Atlantic coast measuring photosynthesis and dark respiration. It was suggested that high-temperature tolerance of the potential warm-adapted macrophytes appeared to be due to genetic adaptation and was likely to be crucial to the persistence of the species near its southern boundary (Gerard and Du Bois 1988). Similar to these studies on macrophytes, I found that Bergen strains had a higher photosynthetic efficiency of PSII at culturing conditions in 8°C than Azores strains. This may indicate that Azores strains are less photosynthetically efficient at low temperatures and hints the presence of ecotype specialization. It was especially interesting that in the southern population, variation in Φ_{PSII} was high between isolates, showing that strains reacted different to temperature stress. Some were more able to manage the temperature than others, which was also reflected in their growth rates. Variation between Bergen strains was smaller at 8°C, however it was higher at 22°C. Combining these findings with the expression of RB, a gene from the small subunit of the enzyme ribulose-1,5-biphosphate carboxylase-oxygenase (RuBisCO), there might be a link to the phenotype. The efficiency of photosynthesis is controlled by temperature-dependent enzymatic steps of the Calvin cycle. Reducing equivalents and ATP are transferred from the light- to the dark cycle where carbon gets fixed. When enzyme reactions of the Calvin cycle are slowed due to low temperatures, the electron transport has to be down-regulated. In this case excitation energy is dissipated non-photochemically.

Maybe beneficial mutations in the Bergen strains resulted in enzymes which help them maintaining the photosynthetic efficiency of PSII at low temperatures. As Azores might not have these alleles, their carbon fixation capacities are slowed down at low temperatures. A possible explanation of the higher regulation of RB at 8°C could be that Azores strains try to counteract the low growth rates by increasing photosynthetic carbon fixation capacities. This may be a response to counteract a bottleneck in carbon fixation. It is known that cellular responses in light variation include an adjustment in the content of RuBisCO (Fisher et al. 1989), so it seems reasonable that a modulation in the RuBisCO content can also occur in temperature changes to increase photosynthetic rates. Overall, genes were more up-regulated in the warmer treatment, probably due to higher metabolic rates. To investigate the expression of Heat shock proteins would have been very interesting as they are produced when an organism is exposed to stressful temperatures. The threshold that defines when a temperature becomes stressful varies among species and is correlated with the conditions the species is adapted and acclimated to (Schlichting and Pigliucci 1995). Gene expression was used to get insights on the molecular phenotype. However, it must be noted that due to high standard deviations between technical replicates, the interpretations of the gene expression results should be regarded with constraints (see 2.5.5).

Next, I looked at how the measured parameters interacted with each other. The correlation of $\Delta F/F_m'$ and growth rate μ was high for the 8°C measurements ($R^2= 0.63$), showing a direct relationship between photosynthetic efficiency and growth. Contrasting to the finding for 8°C, at 22°C no correlation could be found which might be due to light-limitation. As indicated before, photosynthesis is temperature-dependent. Carbon can be fixed only as fast as the enzymes work. At high temperatures enzyme reactions are faster, so carbon fixation depends on the energy amount in form of light. Light curves conducted in a pre-experiment are supporting this idea, in which photosynthesis was light-saturated at actinic light intensities of approximately 600 $\mu\text{mol}/\text{m}^2\cdot\text{sec}$ PAR at 22°C.

I found a negative linear relationship between growth rate and size. This relationship indicates that fixed carbon is either invested in cell size or in dividing faster. When the effective quantum yields were low, the growth rates were also low. Combining this finding with the correlation of growth and size, results indicate that when photosynthetic efficiency is low, the cells may not divide that often and become bigger. As the particle counter only measures coccosphere diameter, it cannot be distinguished whether the cell size or the

coccosphere is bigger. To prove this, PIC and POC measurements would have been needed. They are used to estimate carbon fixation and calcification rates. Further, a decreasing size with increasing growth rate at increasing temperatures was found. Also Sorrosa (2005) found that cell size of *E. huxleyi* and *Gephyrocapsa oceanica* was inversely correlated with increasing temperature and supposed that low temperature suppressed coccolithophorid growth rate but induced cell enlargement and stimulated the intracellular calcification. One of the universal ecological responses to climate warming is supposed to be reduced body size, as detected in a meta-analysis of ectotherm marine organisms (bacteria, phyto- and zooplankton, fish) (Daufresne et al. 2009). My findings are in line with this hypothesis, with the extension that the magnitude of size changes might be population dependent. However, cell division cycles have been found to be synchronized in cultured *E. huxleyi* cells (Müller et al. 2008). As I always measured cell size at the same time, findings could result from Azores strains dividing after the time I counted, while the Bergen strains just divided before.

4.3 Within-population variation

Strain variation was compared between and within the populations to assess the phenotypic plasticity of strains and overall between populations. Variability between strains was highly dependent on temperature and origin, while it was low between strain replicates (showing culturing and measurements to be precise). In the growth rate measurements at 22°C, overall variation was higher in the Bergen group than in the Azores group, while at 8°C the pattern was inverted. Variation was higher in the treatment denoted as the non-native in comparison to the native in growth rate and chlorophyll fluorescence measurements. Simulations have shown that adaptive plasticity buffers variation in a predictable environment, but increases fluctuations in a non-predictable environment (Reed et al. 2010). Findings here would thus indicate adaptive plasticity, because variation was higher in the non-native treatments which represent the less predictable environments than of the more predictable 'native' environments. The higher variation in the non-native temperature regime indicated different levels of temperature-related fitness between the strains. To see whether these differences in performance of strains were compensated by a better or worse performance in the other treatment, linear reaction norms were implemented. Reaction norms can be conducted for individuals to measure the plasticity and genotype-by-environment interactions, as well as for populations by comparing the mean of individual genotype responses to compare population-by-environment interactions (e.g. Kawecki and

Ebert 2004, Pigliucci 2005, Thompson 1991). Overall, the Bergen population showed a lower plasticity through a smaller response to environmental variation than the Azores population on growth. On the first view, this deviated from the expectation of showing higher plasticity, but resulted from a higher fitness in both temperature regimes. By maintaining fitness relative to that of the Azores population, this could be a sign of adaptive plasticity and homeostasis of the Bergen population (Thompson 1991). Homeostasis is defined as “the property of an organism to adjust itself to variable conditions, or self regulatory mechanisms of the organism which permit it to stabilize itself in fluctuating inner and outer environments” (Lerner 1954). It may be important in the role of evolutionary responses of a genotype in relation to environmental variation (Thompson 1991). The Bergen population showed a greater capacity to buffer environmental stress, which is reasonable as they are naturally encountered to greater temperature fluctuations. This might be true for a certain temperature range, but as noted before, Bergen strains suffer earlier from higher temperatures than Azores strains (Yong Zhang, personal communication).

Genotype-by-environment interactions could be detected on the strain level. As the genotypes had reaction norms with different slopes, and were sometimes crossing, it would not have been possible to predict a ranking order of genotype performance from one temperature to the other. Contrasting to the results of Gsell et al. (2012) in which they compared strains of the diatom *Asterionella formosa* from two different habitats in reaction norms, I found a genotype from the southern location performing best in comparisons to the other strains of same origin in both temperatures (A6/M10). A genotype may perform best in a certain set of environments, but usually performs less well than other genotypes in a different environment (reviewed in Richards et al. 2006). Without costs and constraints on plasticity, a genotype producing a locally optimal phenotype would become dominant in a population (Kawecki and Ebert 2004). The most important G x E interaction for local adaptation is thought to be antagonistic pleiotropy, by which alleles have opposite effects on fitness in different habitats (Kawecki and Ebert 2004). Such antagonistic pleiotropy implies that no single genotype is superior in all habitats. As I only measured the response of temperature, the strain may perform worse to a different environmental parameter. However, G x E interactions were also found in studies with other, mainly more complex organisms, e.g. *Chlamydomonas* (Bell 1991), *Daphnia* (Giebelhausen and Lampert 2001, Mitchell and Lampert 2000), *Drosophila* (Delpuech et al. 1995), medaka fish (Yamahira et al.

2007), and *Arabidopsis* (Pigliucci and Schlichting 1996). Genotype-by-environment interactions in the dinoflagellate *Prorocentrum micans* from two different origins were higher pronounced from strains of the Gulf of Maine than those from George's Bank (Brand 1985). I found G x E interactions to be equally pronounced in both populations. G x E interactions were also found in co-occurring strains of the diatom *Asterionella formosa*, where it was suggested that this contributes to the maintenance of clonal diversity within phytoplankton blooms (Gsell et al. 2012). I found these G x E interactions also within populations of *E. huxleyi*, which are in line with this hypothesis.

Also the gene expression analysis revealed G x E interactions and different expression patterns among populations. The transcription rate of a gene can vary (as seen in some genes between populations) such that it appears to be an adaptive phenotype (Pavey et al. 2008). With the design used in this study, it is possible to grow the same strain under different conditions, and a direct comparison of the responses from a genotype under different environmental conditions can be made. Therefore, it principally allows the assumption of a diverged heritable gene regulation between the populations. Population differences in gene expression within this study were not pronounced. It is possible that there were differences which could just not be detected due to the high standard deviations of technical replicates. Differences between populations have been found in killifish (*Fundulus heteroclitus*) by salinity-dependent patterns of gene expression (Whitehead et al. 2011, 2012). The authors concluded that the gene expression of these genes appear to have diverged by adaptive evolutionary mechanisms among populations. Patterns of the few candidate genes used here were not that clear, but indications for such a divergence could be obtained in some genes by population-and treatment specific responses. In *E. huxleyi*, different properties of regulating gene expression in haploid and diploid cells were found that are evolved in the (temporal) environment they typically inhabit (Rokitta et al. 2011). As genes could not directly be related to a morphotype this is difficult to prove here, but differences in gene regulation between populations occurred. These differences could indicate that gene expression might be heritable or that cells have to adjust or compensate differently due to their genetic entity. As results have to be taken with constraints, this is only very speculative.

4.4 Role of plasticity on marine phytoplankton

Phenotypic plasticity and genetic evolution are two important components for functioning of phytoplankton communities (Chevin et al. 2012). So far, only little concern has been given on these components on marine phytoplankton. With average mutation rates of 10^{-6} per locus/generation, large population size in combination with short generation times, phytoplankton is supposed to adapt among the first to climate change in ocean communities (Gabriel and Lynch 1992). Due to its mostly asexual reproduction and only rare sexual events (Rynearson and Armbrust 2005), it has been questioned why there is still such a high genetic diversity maintained. In periods of asexual reproduction, fitness differences among clones can rapidly change genotypic frequencies. However, genetic diversity was found to be maintained during a diatom bloom (Rynearson and Armbrust 2005). An explanation why there is so much genotypic variation in blooms of phytoplankton may be the enormous clonal diversity due to past sexual reproduction events in combination with frequent changes in the environments that prevent individual clonal lineages to become dominant (Rynearson and Armbrust 2005). In concordance with other studies, I observed differences between strains from different origins. The variation between populations was found to be higher than the variation within populations. This fits well to the microsatellite data that indicated limited gene flow, which is a pre-requisite for local adaptation. Thus local adaptation in *E. huxleyi* appears likely. Taking into account that the strains in their natural environment are exposed to different temperature conditions, divergence through ecotype speciation is likely. Comparisons of populations revealed differentiation in both phenotypic responses and genetic data. The findings contrast the “everything-is-everywhere” idea by Finlay, which comprises that microbial species can potentially disperse everywhere due to rarely being restricted by geographical barriers. Persistent restricted gene flow based on geographically separation may lead to population differentiation and high diversity in planktonic organisms, despite the effect of their large population sizes and almost ubiquitous distribution (Casteleyn et al. 2010).

I found genotype-by-environment interactions in both populations for growth rates and gene expression in reaction norms. Genotype-by-environment interactions indicated the presence and importance of high standing genetic variation. Such high standing genetic variation is likely to be important for populations in changing environments. High standing genetic variation enhances the potential for fast adaptation on environmental changes,

because pre-adapted genotypes are likely to be among present genotypes. Phenotypic plasticity may be an adaptive strategy as it allows genotypes to cope with a range of environments (Gsell et al. 2012). Dependent on the selection pressure different populations are encountered to, the amount of plasticity can evolve differently between populations (Aubin-Horth and Renn 2009). Thus, phenotypic plasticity might be important for natural *E. huxleyi* populations under different environmental conditions. If phytoplankton populations, as seen here, show different capacities to buffer changing environments, this could also lead to differential fast responses to e.g. ocean acidification between populations. There is increasing evidence that suggest phenotypic plasticity to be important for organisms to adapt to climate change (Merilä 2012). In this study, evolved phenotypic plasticity was detected. Plasticity buffers fitness to a certain degree, but climate change might exceed these thresholds (Gabriel and Lynch 1992). Anyway, by adding phenotypic mechanisms into models, it may improve the ability to predict population responses to climate change (Reed et al. 2010). As I found high variation between strains of the same location, it underlines the difficulty in predicting ecological dynamics and future ocean scenarios. Many studies used only a single strain, although it was already supposed to use more strains in 1992 (Wood and Leatham 1992). There is a risk to translate these single strain responses to a general response of *E. huxleyi* to climate change. De Bodt et al. (2010) used only one *E. huxleyi* strain, where he found interactive effects of pCO₂ and temperature on calcification. Feng et al. (2008) used only one strain from the Sargasso Sea to test for the interactive effects of pCO₂, temperature, and irradiance. Langer et al. (2009) already saw the importance of strain-specific responses and tested four strains to changing seawater carbonate chemistry. The strains originated from different parts of the world. But also here, he used only one strain from each location. Here, I expand the idea to use not only isolates from different locations, but also more than one strain from each location.

5. Conclusions

Within this study, I found that between-population differentiation is higher than within-population variation of *Emiliana huxleyi* strains from two different geographical origins. Restricted gene flow was identified by microsatellite analysis, such that these strains were shown to come from two distinct populations. These results may contradict the everything-is-everywhere hypothesis by Finlay which implies that no biogeographic patterns exist (1999, 2002). Growth rate measurements as fitness proxy revealed no significant disparity in the warm temperature, but a significantly higher fitness of the northern population in the cold treatment. Thus, local temperature adaptation according to temperature of geographic origin is likely. To verify this suggestion, further populations need to be tested (Kawecki and Ebert 2004). Measurements on growth rate and photosynthetic efficiency under culturing conditions were in concordance by showing the same picture. A correlation of growth rate and effective quantum yield of PSII was found for 8°C which showed a direct relationship between photosynthetic efficiency and growth, while at 22°C photosynthesis might be limited by light availability. There was a linear negative relationship between growth rates and size as found in previous studies. Additionally, a general pattern in size was found as the Azores strains were generally bigger. Furthermore, the growth rate and effective quantum yield of PSII responses revealed higher variations between strains in the 'non-native' treatment which indicated adaptive phenotypic plasticity. Reaction norms of growth rate obtained adaptive phenotypic plasticity, as the Bergen population was able to maintain higher fitness relative to that of the Azores population in both temperature conditions. The populations might thus have a different potential to buffer environmental fluctuations. Although showing no clear divergence (and RT-qPCR results have to be regarded with constraints, see 2.5.5), in some genes population-and treatment-specific differences were obtained in transcriptional regulation. Genotype-by-environment interactions were detected in responses to both, growth rates and gene expression, indicating the presence of high standing genetic variation. High standing genetic variation and phenotypic plasticity are prerequisites for fast responses to changing environmental conditions. Thus, my results support the idea that high standing genetic variation and phenotypic plasticity may be important mechanisms for adaptive evolution in natural *E. huxleyi* populations. Including this phenotype plasticity information into models could improve the ability to predict how *E. huxleyi* will respond to future ocean conditions. Finally, this study underlines the importance to use more than one strain in studies, especially when responses are used for predictions.

References

- Agrawal AA. 2001. Phenotypic plasticity in the interactions and evolution of species. *Science* 294: 321-326.
- Armstrong RA, Peterson ML, Lee C, Wakeham SG. 2009. Settling velocity spectra and the ballast ratio hypothesis. *Deep Sea Research Part II: Topical Studies in Oceanography* 56: 1470-1478.
- Armstrong RA, Lee C, Hedges JI, Honjo S, Wakeham SG. 2001. A new, mechanistic model for organic carbon fluxes in the ocean based on the quantitative association of POC with ballast minerals. *Deep Sea Research Part II: Topical Studies in Oceanography* 49: 219-236.
- Aubin-Horth N, Renn SCP. 2009. Genomic reaction norms: using integrative biology to understand molecular mechanisms of phenotypic plasticity. *Molecular ecology* 18: 3763-3780.
- Bach LT, Riebesell U, Georg Schulz K. 2011. Distinguishing between the effects of ocean acidification and ocean carbonation in the coccolithophore *Emiliana huxleyi*. *Limnology and Oceanography* 56: 2040-2050.
- Barrett RDH, Schluter D. 2008. Adaptation from standing genetic variation. *Trends in Ecology & Evolution* 23: 38-44.
- Beardall J, Raven JA. 2004. The potential effects of global climate change on microalgal photosynthesis, growth and ecology. *Phycologia* 43: 26-40.
- Belkhir K, Borsa P, Chikhi L, Raufaste N, Catch F. 2004. GENETIX 4.05, software under Windows for the genetics of populations. University of Montpellier, Montpellier, France.
- Bell G. 1991. The ecology and genetics of fitness in *Chlamydomonas* III. Genotype-by-environment interaction within strains. *Evolution* 45: 668-679.
- Bijma J, Altabet M, Conte M, Kinkel H, Versteegh G, Volkman J, Wakeham S, Weaver P. 2001. Primary signal: Ecological and environmental factors-Report from Working Group 2. *Geochemistry geophysics geosystems*, 2GC000051 2000.
- Bindoff NL, Willebrand J, Artale V, Cazenave A, Gregory JM, Gulev S, Hanawa K, Le Quere C, Levitus S, Nojiri Y. 2007. Observations: oceanic climate change and sea level.
- Bradbury M, Baker NR. 1981. Analysis of the Slow Phases of the In vivo Chlorophyll Fluorescence Induction Curve - Changes in the Redox State of Photosystem-II Electron-Acceptors and Fluorescence Emission from Photosystem-I and Photosystem-II. *Biochimica Et Biophysica Acta* 635: 542-551.
- Bradshaw. 1965. Evolutionary significance of phenotypic plasticity in plants. *Advances in genetics* 13: 115-155.
- Bradshaw, Holzapfel C. 2007. Genetic response to rapid climate change: it's seasonal timing that matters. *Molecular ecology* 17: 157-166.
- Brand LE. 1982. Genetic variability and spatial patterns of genetic differentiation in the reproductive rates of the marine coccolithophores *Emiliana huxleyi* and *Gephyrocapsa oceanica*. *Limnology and Oceanography* 27: 236-245.

- Brand LE. 1985. Low genetic variability in reproduction rates in populations of *Prorocentrum micans* Ehrenb.(Dinophyceae) over Georges bank. *Journal of Experimental Marine Biology and Ecology* 88: 55-65.
- Bruhn A, LaRoche J, Richardson K. 2010. *Emiliana huxleyi* (Prymnesiophyceae): Nitrogen-metabolism genes and their their expression in response to external nitrogen sources *Journal of Phycology* 46: 266-277.
- Buitenhuis ET, van der Wal P, de Baar HJW. 2001. Blooms of *Emiliana huxleyi* are sinks of atmospheric carbon dioxide: A field and mesocosm study derived simulation. *Global Biogeochem. Cycles* 15: 577-587.
- Buitenhuis ET, Pangerc T, Franklin DJ, Le Quéré C, Malin G. 2008. Growth rates of six coccolithophorid strains as a function of temperature. *Limnology and Oceanography* 53: 1181-1185.
- Bustin SA. 2000. Absolute quantification of mRNA using real-time reverse transcription polymerase chain reaction assays. *Journal of molecular endocrinology* 25: 169-193.
- Butler WL. 1978. Energy-Distribution in Photo-Chemical Apparatus of Photosynthesis. *Annual Review of Plant Physiology and Plant Molecular Biology* 29: 345-378.
- Casteleyn G, Leliaert F, Backeljau T, Debeer AE, Kotaki Y, Rhodes L, Lundholm N, Sabbe K, Vyverman W. 2010. Limits to gene flow in a cosmopolitan marine planktonic diatom. *Proceedings of the National Academy of Sciences* 107: 12952-12957.
- Chevin LM, Lande R, Mace GM. 2012. Adaptation, plasticity, and extinction in a changing environment: towards a predictive theory. *Functional Ecology* 8.
- Collins S, Bell G. 2004. Phenotypic consequences of 1,000 generations of selection at elevated CO₂ in a green alga. *Nature* 431: 566-569.
- Conte MH, Thompson A, Lesley D, Harris RP. 1998. Genetic and physiological influences on the alkenone/alkenoate versus growth temperature relationship in *Emiliana huxleyi* and *Gephyrocapsa oceanica*. *Geochimica et Cosmochimica Acta* 62: 51-68.
- Cook SS, Whittock L, Wright SW, Hallegraeff GM. 2011. Photosynthetic pigment and genetic differences between two southern morphotypes of *Emiliana huxleyi* (Haptophyta). *Journal of Phycology* 47: 615-626.
- Crispo E. 2008. Modifying effects of phenotypic plasticity on interactions among natural selection, adaptation and gene flow. *Journal of Evolutionary Biology* 21: 1460-1469.
- Daufresne M, Lengfellner K, Sommer U. 2009. Global warming benefits the small in aquatic ecosystems. *Proceedings of the National Academy of Sciences* 106: 12788-12793.
- De Bodt C, Van Oostende N, Harlay J, Sabbe K, Chou L. 2010. Individual and interacting effects of pCO₂ and temperature on *Emiliana huxleyi* calcification: study of the calcite production, the coccolith morphology and the coccosphere size. *Biogeosciences* 7: 1401-1412.

- De Boer MK, Koolmees EM, Vrieling EG, Breeman AM, Van Rijssel M. 2005. Temperature responses of three *Fibrocapsa japonica* strains (Raphidophyceae) from different climate regions. *Journal of plankton research* 27: 47-60.
- De Jong G. 1990. Quantitative genetics of reaction norms. *Journal of Evolutionary Biology* 3: 447-468.
- Delille B, Harlay J, Zondervan I, Jacquet S, Chou L, Wollast R, Bellerby RGJ, Frankignoulle M, Borges AV, Riebesell U. 2005. Response of primary production and calcification to changes of pCO₂ during experimental blooms of the coccolithophorid *Emiliana huxleyi*. *Global Biogeochemical Cycles* 19: GB2023.
- Delpuech JM, Moreteau B, Chiche J, Pla E, Vouidibio J, David JR. 1995. Phenotypic plasticity and reaction norms in temperate and tropical populations of *Drosophila melanogaster*: ovarian size and developmental temperature. *Evolution*: 670-675.
- Dickson A, Whitfield M, Turner D. 1981. Concentration products: their definition, use and validity as stability constants. *Marine Chemistry* 10: 559-565.
- Dickson AG, Sabine CL, Christian JR. 2007. Guide to best practices for ocean CO₂ measurements. PICES special publication 3: 191pp.
- Doney SC, Schimel DS. 2007. Carbon and Climate System Coupling on Timescales from the Precambrian to the Anthropocene. *Annu. Rev. Environ. Resour.* 32: 31-66.
- Doney SC, Fabry VJ, Feely RA, Kleyvas JA. 2009. Ocean acidification: the other CO₂ problem. *Marine Science* 1.
- Doney SC, Ruckelshaus M, Duffy JE, Barry JP, Chan F, English CA, Galindo HM, Grebmeier JM, Hollowed AB, Knowlton N. 2012. Climate change impacts on marine ecosystems. *Marine Science* 4.
- Egge J, Aksnes D. 1992. Silicate as regulating nutrient in phytoplankton competition. *Marine ecology progress series*. Oldendorf 83: 281-289.
- Eggert A, Van Hasselt P, Breeman A. 2003. Differences in thermal acclimation of chloroplast functioning in two ecotypes of *Valonia utricularis* (Chlorophyta). *European Journal of Phycology* 38: 123-131.
- Engel A, et al. 2005. Testing the direct effect of CO₂ concentration on a bloom of the coccolithophorid *Emiliana huxleyi* in mesocosm experiments. *Limnology and Oceanography*: 493-507.
- Excoffier L, Laval G, Schneider S. 2005. Arlequin (version 3.0): an integrated software package for population genetics data analysis. *Evolutionary bioinformatics online* 1: 47-50.
- Ezard THG, Côté SD, Pelletier F. 2009. Eco-evolutionary dynamics: disentangling phenotypic, environmental and population fluctuations. *Philosophical Transactions of the Royal Society B: Biological Sciences* 364: 1491-1498.
- Falkowski PG, Katz ME, Knoll AH, Quigg A, Raven JA, Schofield O, Taylor F. 2004. The evolution of modern eukaryotic phytoplankton. *Science* 305: 354-360.

- Feely RA, Sabine CL, Takahashi T, Wanninkhof R. 2001. Uptake and storage of carbon dioxide in the ocean. *Oceanography* 14: 18-32.
- Feely RA, Sabine CL, Lee K, Berelson W, Kleypas J, Fabry VJ, Millero FJ. 2004. Impact of anthropogenic CO₂ on the CaCO₃ system in the oceans. *Science* 305: 362-366.
- Feng Y, Warner ME, Zhang Y, Sun J, Fu FX, Rose JM, Hutchins DA. 2008. Interactive effects of increased pCO₂, temperature and irradiance on the marine coccolithophore *Emiliana huxleyi* (Prymnesiophyceae). *European Journal of Phycology* 43: 87-98.
- Finlay BJ. 2002. Global dispersal of free-living microbial eukaryote species. *Science* 296: 1061-1063.
- Finlay BJ, Clarke KJ. 1999. Ubiquitous dispersal of microbial species. *Nature* 400: 828-828.
- Fisher T, Shurtz-Swirski R, Gepstein S, Dubinsky Z. 1989. Changes in the Levels of Ribulose-1, 5-bisphosphate Carboxylase/Oxygenase (Rubisco) in *Tetraedron minimum* (Chlorophyta) during Light and Shade Adaptation. *Plant and cell physiology* 30: 221-228.
- Furnas MJ. 1990. In situ growth rates of marine phytoplankton: approaches to measurement, community and species growth rates. *Journal of plankton research* 12: 1117-1151.
- Gabriel W, Lynch M. 1992. The selective advantage of reaction norms for environmental tolerance. *Journal of Evolutionary Biology* 5: 41-59.
- Genty B, Briantais JM, Baker NR. 1989. The relationship between the quantum yield of photosynthetic electron transport and quenching of chlorophyll fluorescence. *Biochimica et Biophysica Acta (BBA)-General Subjects* 990: 87-92.
- Gerard V, Du Bois K. 1988. Temperature ecotypes near the southern boundary of the kelp *Laminaria saccharina*. *Marine Biology* 97: 575-580.
- Gibson U, Heid CA, Williams PM. 1996. A novel method for real time quantitative RT-PCR. *Genome research* 6: 995-1001.
- Giebelhausen B, Lampert W. 2001. Temperature reaction norms of *Daphnia magna*: the effect of food concentration. *Freshwater Biology* 46: 281-289.
- Green J, Course P, Tarran G. 1996. The life-cycle of *Emiliana huxleyi*: A brief review and a study of relative ploidy levels analysed by flow cytometry. *Journal of marine systems* 9: 33-44.
- Gsell AS, Senerpont Domis LN, Przytulska-Bartosiewicz A, Mooij WM, Donk E, Ibelings BW. 2012. Genotype-by-Temperature Interactions may Help to Maintain Clonal Diversity in *Asterionella Formosa* (Bacillariophyceae). *Journal of Phycology*.
- Guillard RRL, Ryther JH. 1962. Studies of marine planktonic diatoms: I. *Cyclotella nana* Hustedt, and *Detonula confervacea* (Cleve) Gran. *Canadian journal of microbiology* 8: 229-239.
- Higuchi R, Dollinger G, Walsh PS, Griffith R. 1992. Simultaneous amplification and detection of specific DNA sequences. *Bio/Technology* 10: 413-417.
- Higuchi R, Fockler C, Dollinger G, Watson R. 1993. Kinetic PCR analysis: real-time monitoring of DNA amplification reactions. *Biotechnology* 11: 1026-1030.

- Hofmann GE, Barry JP, Edmunds PJ, Gates RD, Hutchins DA, Klinger T, Sewell MA. 2010. The effect of ocean acidification on calcifying organisms in marine ecosystems: an organism-to-ecosystem perspective. *Annual review of ecology, evolution, and systematics* 41: 127-147.
- Honjo S, Manganini SJ, Cole JJ. 1982. Sedimentation of biogenic matter in the deep ocean. *Deep Sea Research Part A. Oceanographic Research Papers* 29: 609-625.
- Hurrell JW. 1995. Decadal trends in the North Atlantic Oscillation: regional temperatures and precipitation. *Science* 269: 676-679.
- Iglesias-Rodriguez MD, Schofield OM, Batley J, Medlin LK, Hayes PK. 2006. Intraspecific genetic diversity in the marine coccolithophore *Emiliana huxleyi* (Prymnesiophyceae): the use of microsatellite analysis in marine phytoplankton population studies. *J. Phycol* 42: 526-536.
- Iglesias-Rodriguez MD, Saez AG, Groben R, Edwards KJ, Batley J, Medlin LK, Hayes PK. 2002. Polymorphic microsatellite loci in global populations of the marine coccolithophorid *Emiliana huxleyi*. *Molecular Ecology Notes* 2: 495-497.
- IPCC CC. 2007. Synthesis report. IPCC, Geneva, Switzerland 104.
- Ittekkot V. 1993. The abiotically driven biological pump in the ocean and short-term fluctuations in atmospheric CO₂ contents. *Global and Planetary Change* 8: 17-25.
- JMP S. 2007. Version 7. Cary: SAS Institute Inc: 1989-2007.
- Jordan RW, Cros L, Young JR. 2004. A revised classification scheme for living haptophytes. *Micropaleontology* 50: 55-79.
- Kaufman JA. 2007. Studies of marine calcification: Calcification capacity and genetic responses to nutrient limitation and stress in *Emiliana huxleyi* (Haptophyta) University of California, Los Angeles.
- Kawecki TJ, Ebert D. 2004. Conceptual issues in local adaptation. *Ecology letters* 7: 1225-1241.
- Krause GH, Weis E. 1984. Chlorophyll Fluorescence as a Tool in Plant Physiology .2. Interpretation of Fluorescence Signals. *Photosynthesis Research* 5: 139-157.
- Krause GH, Weis E. 1991. Chlorophyll Fluorescence and Photosynthesis - the Basics. *Annual Review of Plant Physiology and Plant Molecular Biology* 42: 313-349.
- Lafon V, Martins A, Figueiredo M, Rodrigues MM, Bashmachnikov I, Mendonca A, Macedo L, Goulart N. 2004. Sea surface temperature distribution in the Azores region. Part I: AVHRR imagery and in situ data processing. *Arquipélago. Life and Marine Sciences*: 1-18.
- Landry CR, Oh J, Hartl DL, Cavalieri D. 2006. Genome-wide scan reveals that genetic variation for transcriptional plasticity in yeast is biased towards multi-copy and dispensable genes. *Gene* 366: 343-351.
- Langer G, Nehrke G, Probert I, Ly J, Ziveri P. 2009. Strain-specific responses of *Emiliana huxleyi* to changing seawater carbonate chemistry. *Biogeosciences* 6: 2637-2646.

- Langer G, Geisen M, Baumann KH, Kläs J, Riebesell U, Thoms S, Young JR. 2006. Species-specific responses of calcifying algae to changing seawater carbonate chemistry. *Geochemistry Geophysics Geosystems*.
- Lerner IM. 1954. Genetic homeostasis. Oliver and Boyd.
- Lewis E, Wallace D. 1998. Program Developed for CO₂ System Calculations (Carbon Dioxide Information Analysis Center, Oak Ridge National Laboratory, US Dept. of Energy, Oak Ridge, TN). ORNL/CDIAC-105. Oak Ridge, Tennessee.
- Li Y, Álvarez OA, Gutteling EW, Tijsterman M, Fu J, Riksen JAG, Hazendonk E, Prins P, Plasterk RHA, Jansen RC. 2006. Mapping determinants of gene expression plasticity by genetical genomics in *C. elegans*. *PLoS genetics* 2: e222.
- Li YC, Korol AB, Fahima T, Beiles A, Nevo E. 2002. Microsatellites: genomic distribution, putative functions and mutational mechanisms: a review. *Molecular ecology* 11: 2453-2465.
- Lohbeck K, Riebesell U, Reusch TBH. 2012. Adaptive evolution of a key phytoplankton species to ocean acidification. *Nature Geoscience* 5.
- Longhurst AR, Glen Harrison W. 1989. The biological pump: profiles of plankton production and consumption in the upper ocean. *Progress in Oceanography* 22: 47-123.
- Mackinder L, Wheeler G, Schroeder D, von Dassow P, Riebesell U, Brownlee C. 2011. Expression of biomineralization-related ion transport genes in *Emiliana huxleyi*. *Environmental Microbiology* 13: 3250-3265.
- Medlin L, Barker G, Campbell L, Green J, Hayes P, Marie D, Wrieden S, Vaultot D. 1996. Genetic characterisation of *Emiliana huxleyi* (Haptophyta). *Journal of marine systems* 9: 13-31.
- Medlin LK. 2007. If everything is everywhere, do they share a common gene pool? *Science direct* 406: 180-183.
- Merilä J. 2012. Evolution in response to climate change: In pursuit of the missing evidence. *BioEssays*.
- Milliman JD. 1993. Production and accumulation of calcium carbonate in the ocean: Budget of a nonsteady state. *Global Biogeochemical Cycles* 7: 927-957.
- Mitchell S, Lampert W. 2000. Temperature adaptation in a geographically widespread zooplankter, *Daphnia magna*. *Journal of Evolutionary Biology* 13: 371-382.
- Müller MN, Antia AN, LaRoche J. 2008. Influence of Cell Cycle Phase on Calcification in the Coccolithophore *Emiliana huxleyi*. *Limnology and Oceanography*: 506-512.
- Mullis K, Faloona F, Scharf S, Saiki R, Horn G, Erlich H. 1986. Specific enzymatic amplification of DNA in vitro: the polymerase chain reaction. Pages 263-273.
- Murata N, Nishimur.M, Takamiya A. 1966. Fluorescence of Chlorophyll in Photosynthetic Systems .2. Induction of Fluorescence in Isolated Spinach Chloroplasts. *Biochimica Et Biophysica Acta* 120: 23-&.
- Nolan T, Hands RE, Bustin SA. 2006. Quantification of mRNA using real-time RT-PCR. *Nature protocols* 1: 1559-1582.

- Oliveira EJ, Pádua JG, Zucchi MI, Vencovsky R, Vieira MLC. 2006. Origin, evolution and genome distribution of microsatellites. *Genetics and Molecular Biology* 29: 294-307.
- Orr JC, Fabry VJ, Aumont O, Bopp L, Doney SC, Feely RA, Gnanadesikan A, Gruber N, Ishida A, Joos F. 2005. Anthropogenic ocean acidification over the twenty-first century and its impact on calcifying organisms. *Nature* 437: 681-686.
- Ozgul A, Childs DZ, Oli MK, Armitage KB, Blumstein DT, Olson LE, Tuljapurkar S, Coulson T. Coupled dynamics of body mass and population growth in response to environmental change. *Nature* 466: 482-485.
- Paasche E. 2001. A review of the coccolithophorid *Emiliana huxleyi* (Prymnesiophyceae), with particular reference to growth, coccolith formation, and calcification-photosynthesis interactions. *Phycologia* 40: 503-529.
- Paasche E, Klaveness D. 1970. A physiological comparison of coccolith-forming and naked cells of *Coccolithus huxleyi*. *Archives of Microbiology* 73: 143-152.
- Palumbi SR. 1994. Genetic divergence, reproductive isolation, and marine speciation. *Annual Review of Ecology and Systematics*: 547-572.
- Parejko K, Dodson SI. 1991. The evolutionary ecology of an antipredator reaction norm: *Daphnia pulex* and *Chaoborus americanus*. *Evolution*: 1665-1674.
- Pavey SA, Collin H, Nosil P, Rogers SM. 2008. The role of gene expression in ecological speciation. *Annals of the New York Academy of Sciences* 1206: 110-129.
- Pigliucci M. 2005. Evolution of phenotypic plasticity: where are we going now? *Trends in Ecology & Evolution* 20: 481-486.
- Pigliucci M, Schlichting CD. 1996. Reaction norms of Arabidopsis. IV. Relationships between plasticity and fitness. *Heredity* 76: 427-436.
- Pritchard JK, Stephens M, Donnelly P. 2000. Inference of population structure using multilocus genotype data. *Genetics* 155: 945-959.
- Quinn P, Bowers RM, Zhang X, Wahlund TM, Fanelli MA, Olszova D, Read BA. 2006. cDNA microarrays as a tool for identification of biomineralization proteins in the coccolithophorid *Emiliana huxleyi* (Haptophyta). *Applied and environmental microbiology* 72: 5512-5526.
- R Development Core Team. 2005. R 2.11.0: R Project for Statistical Computing Vienna, Austria.
- Rainey PB, Buckling A, Kassen R, Travisano M. 2000. The emergence and maintenance of diversity: insights from experimental bacterial populations. *Trends in Ecology & Evolution* 15: 243-247.
- Redfield AC, Ketchum BH, Richards FA. 1963. The influence of organisms on the composition of seawater. *The sea: Ideas and observations on progress in the study of the seas* 2.
- Reed TE, Waples RS, Schindler DE, Hard JJ, Kinnison MT. 2010. Phenotypic plasticity and population viability: the importance of environmental predictability. *Proceedings of the Royal Society B: Biological Sciences* 277: 3391-3400.

- Reusch TBH, Wood TE. 2007. Molecular ecology of global change. *Molecular ecology* 16: 3973-3992.
- Reusch TBH and Boyd PW. 2012. Oceanography - A novel research area for evolutionary biologists. *Evolution*.
- Richards CL, Bossdorf O, Muth NZ, Gurevitch J, Pigliucci M. 2006. Jack of all trades, master of some? On the role of phenotypic plasticity in plant invasions. *Ecology letters* 9: 981-993.
- Richier S, Fiorini S, Kerros ME, Von Dassow P, Gattuso JP. 2011. Response of the calcifying coccolithophore *Emiliana huxleyi* to low pH/high pCO₂: from physiology to molecular level. *Marine Biology* 158: 551-560.
- Richier S, Kerros ME, De Vargas C, Haramaty L, Falkowski PG, Gattuso JP. 2009. Light-dependent transcriptional regulation of genes of biogeochemical interest in the diploid and haploid life cycle stages of *Emiliana huxleyi*. *Applied and environmental microbiology* 75: 3366-3369.
- Rokitta SD, de Nooijer LJ, Trimborn S, de Vargas C, Rost B, John U. 2011. Transcriptome analysis reveal differential gene expression patterns between the life cycle stages of *Emiliana huxleyi* (Haptophyta) and reflect specialization to different ecological niches *Journal of Phycology* 47: 829-838.
- Roy RN, Roy LN, Lawson M, Vogel KM, Porter Moore C, Davis W, Millero FJ. 1993. Thermodynamics of the dissociation of boric acid in seawater at S= 35 from 0 to 55° C. *Marine Chemistry* 44: 243-248.
- Rynearson TA, Armbrust EV. 2000. DNA fingerprinting reveals extensive genetic diversity in a field population of the centric diatom *Ditylum brightwellii*. *Limnology and Oceanography*: 1329-1340.
- Rynearson TA, Armbrust VE. 2004. Genetic differentiation among populations of the planktonic marine diatom *Ditylum brightwellii* (Bacillariophyceae). *Journal of Phycology* 40: 34-43.
- Rynearson TA, Armbrust E. 2005. Maintenance of clonal diversity during a spring bloom of the centric diatom *Ditylum brightwellii*. *Molecular ecology* 14: 1631-1640.
- Sabine CL, Feely RA, Gruber N, Key RM, Lee K, Bullister JL, Wanninkhof R, Wong CS, Wallace DWR, Tilbrook B. 2004. The oceanic sink for anthropogenic CO₂. *Science* 305: 367-371.
- Sarmiento JL, Gruber N. 2006. *Ocean biogeochemical dynamics*: Cambridge Univ Press.
- Savolainen O. 2011. The Genomic Basis of Local Climatic Adaptation. *Science* 334: 49-50.
- Scheiner SM. 1993. Genetics and evolution of phenotypic plasticity. *Annual Review of Ecology and Systematics*: 35-68.
- Schlichting CD, Pigliucci M. 1995. Gene regulation, quantitative genetics and the evolution of reaction norms. *Evolutionary Ecology* 9: 154-168.
- Schlötterer C. 2000. Evolutionary dynamics of microsatellite DNA. *Chromosoma* 109: 365-371.
- Schreiber U, Bilger W, Neubauer C. 1994. Chlorophyll fluorescence as a noninvasive indicator for rapid assessment of in vivo photosynthesis. *Ecological studies: analysis and synthesis* 100.

- Schreiber U, Bilger W, Tenhunen J, Catarino F, Lange O, Oechel W. 1987. Rapid assessment of stress effects on plant leaves by chlorophyll fluorescence measurement. Plant response to stress. Functional analysis in Mediterranean ecosystems.: 27-53.
- Selkoe KA, Toonen RJ. 2006. Microsatellites for ecologists: a practical guide to using and evaluating microsatellite markers. Ecology letters 9: 615-629.
- Sorrosa JM, Satoh M, Shiraiwa Y. 2005. Low temperature stimulates cell enlargement and intracellular calcification of coccolithophorids. Marine Biotechnology 7: 128-133.
- Thierstein HR, Young JR. 2004. Coccolithophores: from molecular processes to global impact: Springer.
- Thierstein HR, Geitzenauer K, Molino B, Shackleton N. 1977. Global synchronicity of late Quaternary coccolith datum levels Validation by oxygen isotopes. Geology 5: 400-404.
- Thompson JD. 1991. Phenotypic plasticity as a component of evolutionary change. Trends in Ecology & Evolution 6: 246-249.
- Tyrrell T, Merico A. 2004. *Emiliana huxleyi*: bloom observations and the conditions that induce them. Coccolithophores: from molecular processes to global impact. Springer-Verlag: 75-97.
- van Bleijswijk J, Wal P, Kempers R, Veldhuis M, Young JR, Muyzer G, de Jong E, Westbroek P. 1991. Distribution of two types of *Emiliana huxleyi* (Prymnesiophyceae) in the northeast atlantic regions as determined by immunofluorescence and coccolith morphology. Journal of Phycology 27: 566-570.
- Via S, Lande R. 1985. Genotype-environment interaction and the evolution of phenotypic plasticity. Evolution: 505-522.
- Weiss RF. 1974. Carbon dioxide in water and seawater: the solubility of a non-ideal gas. Marine Chemistry 2: 203-215.
- Westbroek P, Young J, Linschooten K. 1989. Coccolith production (biomineralization) in the marine alga *Emiliana huxleyi*. Journal of Eukaryotic Microbiology 36: 368-373.
- Whitehead A, Roach JL, Zhang S, Galvez F. 2011. Genomic mechanisms of evolved physiological plasticity in killifish distributed along an environmental salinity gradient. Proceedings of the National Academy of Sciences 108: 6193-6198.
- Whitehead A, Roach JL, Zhang S, Galvez F. 2012. Salinity-and population-dependent genome regulatory response during osmotic acclimation in the killifish (*Fundulus heteroclitus*) gill. The Journal of Experimental Biology 215: 1293-1305.
- Woltereck R. 1913. Weitere experimentelle untersuchungen über Artänderung, speziell über das Wesen quantitativer Artunterschiede bei Daphniden. Molecular and General Genetics MGG 9: 146-146.
- Wood AM, Leatham T. 1992. The species concept in phytoplankton ecology Journal of Phycology 28: 723-729.

- Wright S. 1978. Evolution and the genetics of populations. Variability within and among natural populations. Vol. 4. University of Chicago press, Chicago, IL, USA.
- Yamahira K, Kawajiri M, Takeshi K, Irie T. 2007. Inter- and intrapopulation variation in thermal reaction norms for growth rate: evolution of latitudinal compensation in ectotherms with a genetic constraint. *Evolution* 61: 1577-1589.
- Young JR. 1994. Variation in *Emiliana huxleyi* coccolith morphology in samples from the Norwegian EHUX experiment, 1992. *Sarsia* 79: 417-425.
- Young JR, Westbroek P. 1991. Genotypic variation in the coccolithophorid species *Emiliana huxleyi*. *Marine Micropaleontology* 18: 5-23.
- Zeebe RE, Wolf-Gladrow DA. 2001. CO₂ in seawater: equilibrium, kinetics, isotopes: Elsevier Science Limited.
- Zondervan I, Zeebel RE, Rost B, Riebesell U. 2001. Decreasing marine biogenic calcification: A negative feedback on rising atmospheric pCO₂ *Global Biogeochemical Cycles* 15: 507-516.

Appendix

A CaM and Hsp90

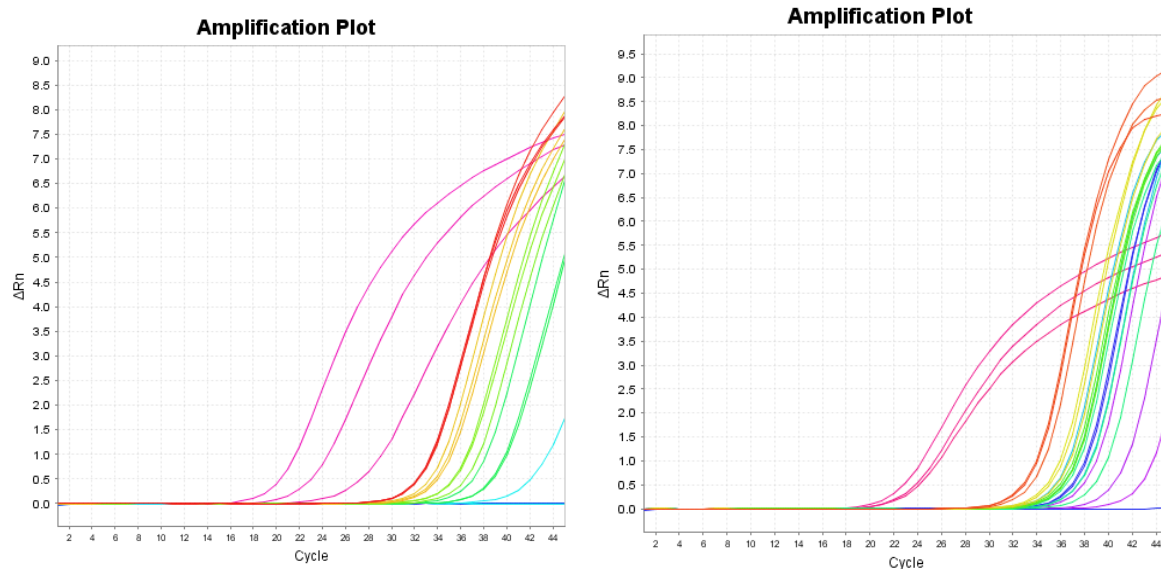


Fig.25: Standard curved of CaM and Hsp90. Left: CaM, right: Hsp90. -RT in pink shows that a product is amplified which is even more occurring than product of the dilution series (other colours).

B Histograms

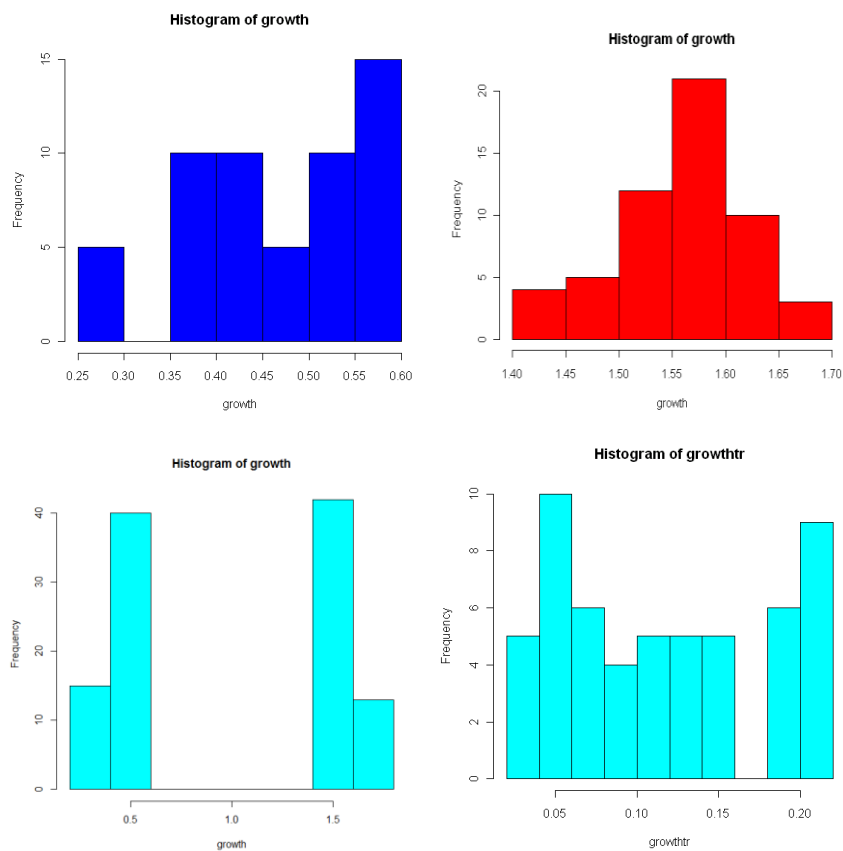
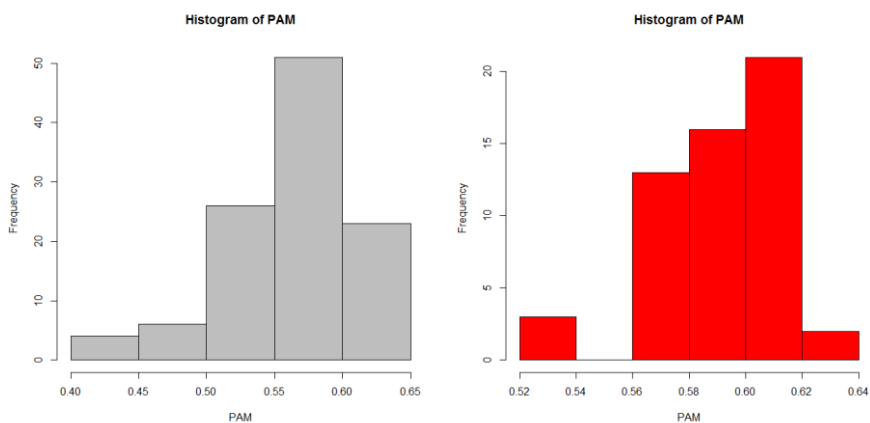


Fig. 26: Histograms of Growth rates. Top, left: 8°C, right: 22°C. Bottom, left: all data, not transformed, right: all data transformed with $\wedge 3$.



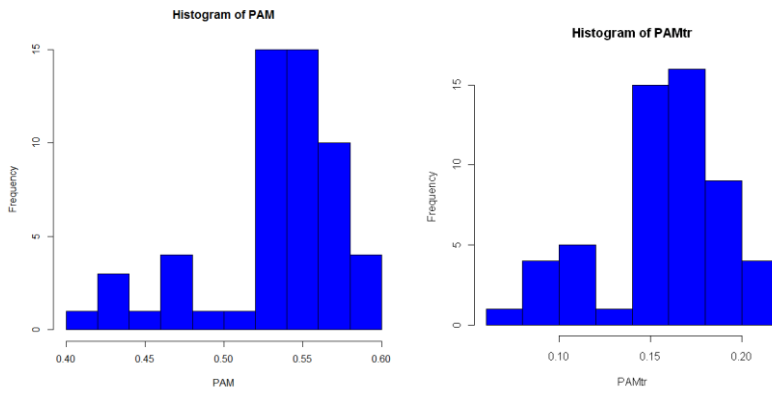


Fig. 27: Histograms of Chlorophyll fluorescence. Top, left: all data, right: 22°C. Bottom, left: 8°C untransformed, right: 8°C transformed with $\wedge 3$.

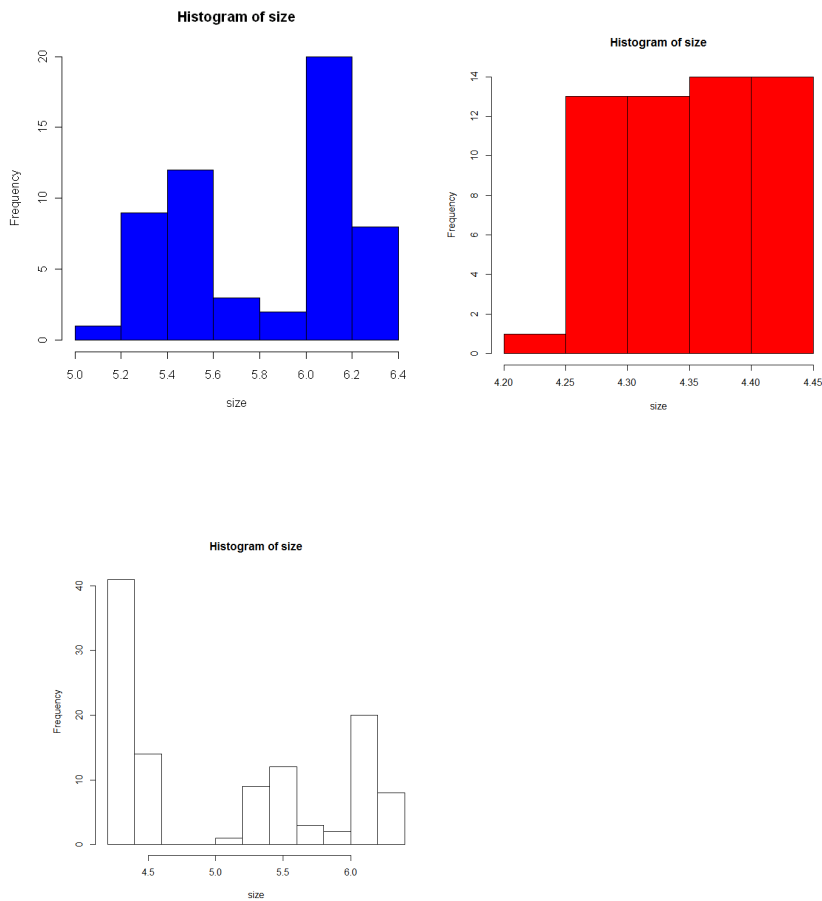


Fig. 28: Histograms of Size. Top, left: Size at 8°C, right: 22°C, Bottom: All

C Microsatellite Primers

Tab. 8: Microsatellite primers for *Emiliana huxleyi*. In this study, primers S15, E9, F08, E10, S37, A08, F11, E5, B12, and E11 were used (Iglesias-Rodriguez et al. 2006).

Locus	Primer sequence	EMBL Access. No	Sequenced repeat motif	T_n	Allele size (bp)	No. alleles	No. genotypes	% Un. Gen.	H_o	H_E	$P_{-val} \pm SE$
<i>EHMS15^b</i> N = 61	F: TCGAGCGCGTCACACAC R: CGGAGCGGTGGCAATGT	AJ487304 AJ487305	(GT) ₂₇ GC	54	72–149	26	38	71.05	0.70*	0.93	0.0068 ± 0.00440
<i>EHMS37</i> N = 35	F: TGTGAGAGTGAGCAGCA R: TTGAGGAGGATACGAGTC	AJ494737 AJ494738	(GT) ₂₃	60	203–240	11	17	70.27	0.58*	0.78	0.0109 ± 0.0021
<i>P01F08^b</i> N = 60	F: CGGAGCATCCAGTACACAA R: CGCATCTCAGTCGTTCTCA	AJ487306 AJ487307	(GT) ₁₄	60	144–198	18	38	61.11	0.75*	0.88	0.0000 ± 0.0000
<i>P02A08^b</i> N = 41	F: CCCGTTGTTTGGAGAGAGA R: TCGGAGATCAGGAGTTGTC	AJ487308 AJ487309	(GA) ₁₆ GG (GA) ₂₃	58	281–331	15	18	70.73	0.34*	0.84	0.0000 ± 0.0000
<i>P02E11^b</i> N = 58	F: CGGTCTACGAGGTGTAA R: CACGGCTTCAAAATGTAAT	AJ487312 AJ487313	(GA) ₇ TA (GA) ₇	58	206–251	21	41	63.63	0.74*	0.92	0.0000 ± 0.0000
<i>P02B12^b</i> N = 50	F: GGTTAATCCAGCAAAGC R: CAGCTTTGATCGGAAACGA	AJ487309 AJ487311	(GT) ₁₀	58	204–220	7	12	60.00	0.40	0.47	0.7479 ± 0.0039
<i>P02E10^b</i> N = 40	F: CTCCTGTAGTCGGGAGTGT R: CACGGTTCAGGAAATACCT	AJ487314 AJ487315	(GT) ₁₁ GCAA(GT) ₁₁	58	164–180	8	11	70.58	0.28*	0.52	0.0104 ± 0.0007
<i>P02F11^b</i> N = 57	F: CACGGTTCAGGAAATACCT R: TCCAAAGCAAAGTCAAAA	AJ487316 AJ487317	(GT) ₁₁	58	100–149	16	18	28.57	0.58	0.67	0.1071 ± 0.0075
<i>P01E05</i> N = 66	F: GTGTGCCCTTTTGTGCTTTT R: GTGATGGTTCCTGCTGTTTC	AJ494739 AJ494740	(GA) ₁₄ GG (GA) ₂₁	57	120–190	26	39	58.82	0.70*	0.92	0.0018 ± 0.0018
<i>P02E09</i> N = 76	F: ACTGGACTGGACGCACA R: GGCTGCTCTTCCCTCTCTA	AJ494741 AJ494742	(GT) ₉	59	82–104	9	14	66.66	0.68	0.69	0.3452 ± 0.0131

^aHeterozygote deficiency.

^bLoci attributes described in Iglesias-Rodriguez et al. (2002).

Access No., Accession Number; T_n , annealing temperature (°C); observed (H_o) and expected (H_E) heterozygosity (calculated as $1 - \sum P_i^2$, where P_i is the frequency of each allele), Un. Gen., unique genotypes. A collection of 85 *E. huxleyi* clonal isolates was used in this study. N , number of isolates with detectable alleles; P_{-val} , significant exact probability (P) for Hardy–Weinberg departure proportions. SE, standard error.

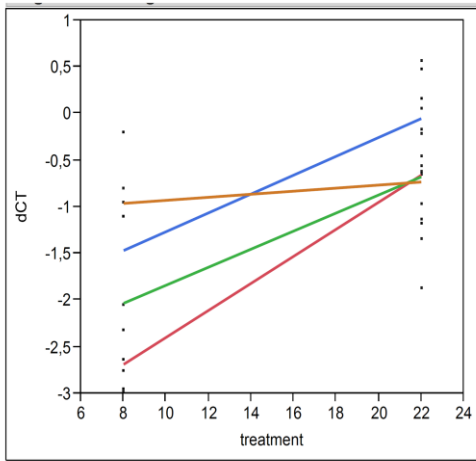
D Carbonate System parameters

Table 9: Carbonate System parameters of the Experiment. DIC and Alkalinity were measured, the other parameters calculated with CO2SYS (Lewis and Wallace 1998).

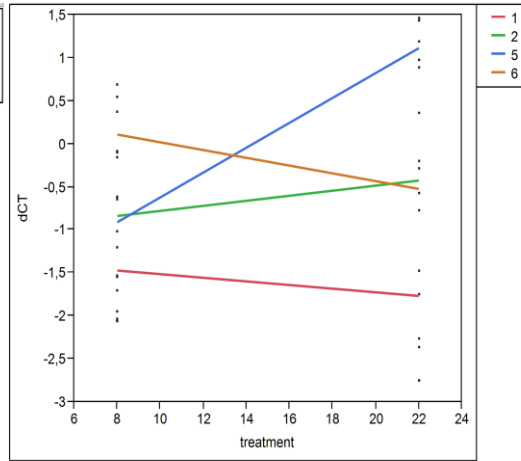
Temp. [°C]	Batch cycle	DIC ($\mu\text{mol/kgSW}$)	TA ($\mu\text{mol/kgSW}$)	DIC ($\mu\text{mol/kgSW}$)	pH	fCO ₂ (μatm)	HCO ₃ ($\mu\text{mol/kgSW}$)	CO ₃ ⁻ ($\mu\text{mol/kgSW}$)	CO ₂ ($\mu\text{mol/kgSW}$)	Ω [Calcite]	Ω [Aragonite]
8°C	09.05.2012	2143.246032	2309.73	2143.246032	8.017	431.4	1999.9	123.1	20.2	2.93	1.86
8°C	20.05.2012	2108.795866	2309.73	2108.795866	8.095	350.7	1948.6	143.8	16.5	3.43	2.17
8°C	20.05.2012	2106.567284	2309.73	2106.567284	8.100	346.2	1945.2	145.1	16.2	3.46	2.19
8°C	25.05.2012	2123.838796	2309.73	2123.838796	8.062	383.2	1971.2	134.6	18.0	3.21	2.03
8°C	31.05.2012	2105.917281	2309.73	2105.917281	8.102	344.9	1944.2	145.5	16.2	3.47	2.20
15°C	27.04.2012	2049.645581	2309.73	2049.645581	8.099	351.9	1851.3	185.2	13.2	4.41	2.83
15°C	27.04.2012	2046.024135	2309.73	2046.024135	8.105	345.5	1845.6	187.5	12.9	4.47	2.87
15°C	29.05.2012	2031.445494	2309.73	2031.445494	8.132	320.9	1822.6	196.8	12.0	4.69	3.01
15°C	29.05.2012	2023.738314	2309.73	2023.738314	8.146	308.8	1810.4	201.8	11.6	4.81	3.09
22°C	06.05.2012	1991.238157	2309.73	1991.238157	8.088	357.2	1753.3	227.0	11.0	5.44	3.56
22°C	12.05.2012	1972.109494	2309.73	1972.109494	8.119	326.8	1722.6	239.5	10.0	5.74	3.75
22°C	03.06.2012	1975.545225	2309.73	1975.545225	8.113	332.0	1728.1	237.3	10.2	5.69	3.72
22°C	05.06.2012	1975.73094	2309.73	1975.73094	8.113	332.3	1728.4	237.1	10.2	5.68	3.71

E Reaction norms gene expression

ATPc/c'

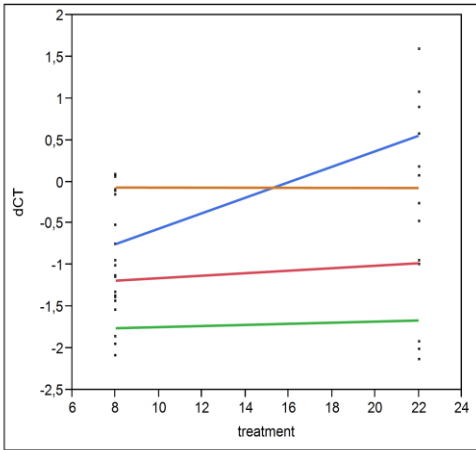


Bergen

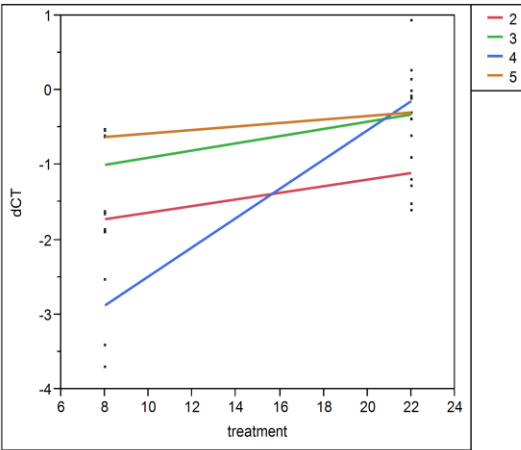


Azores

CAX3

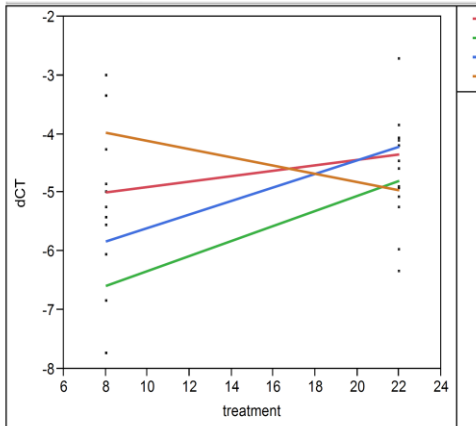


Bergen

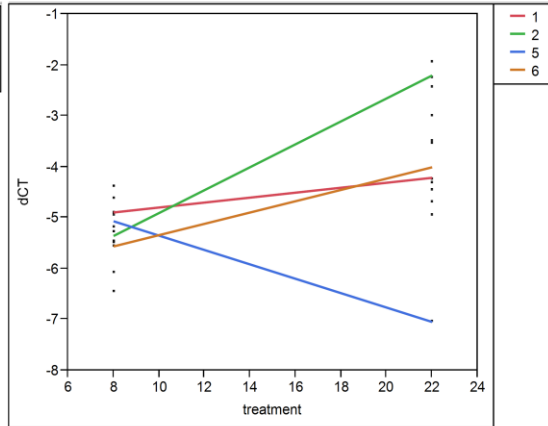


Azores

GPA

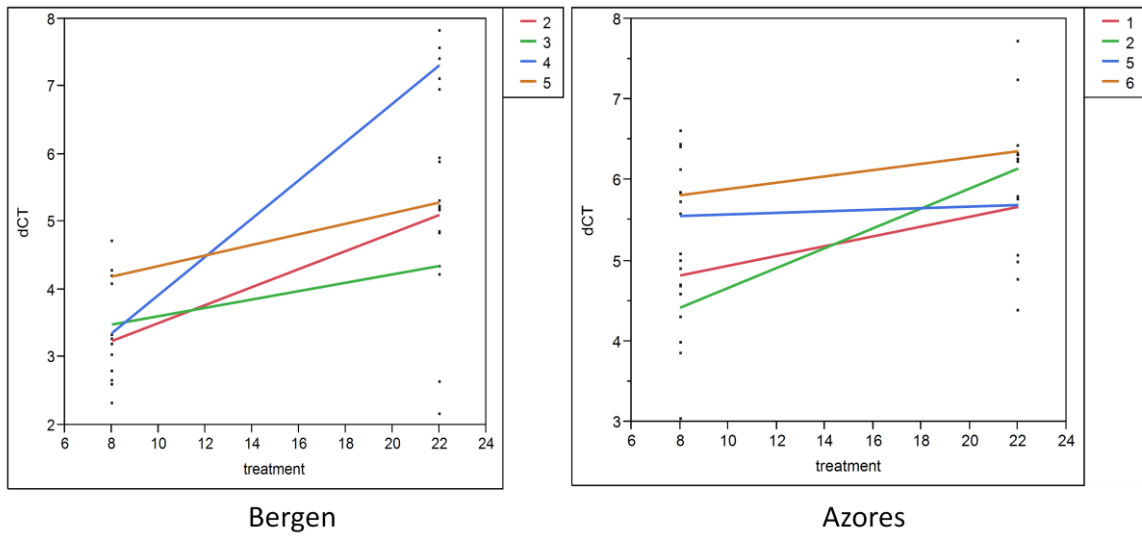


Bergen



Azores

RB



SLC4

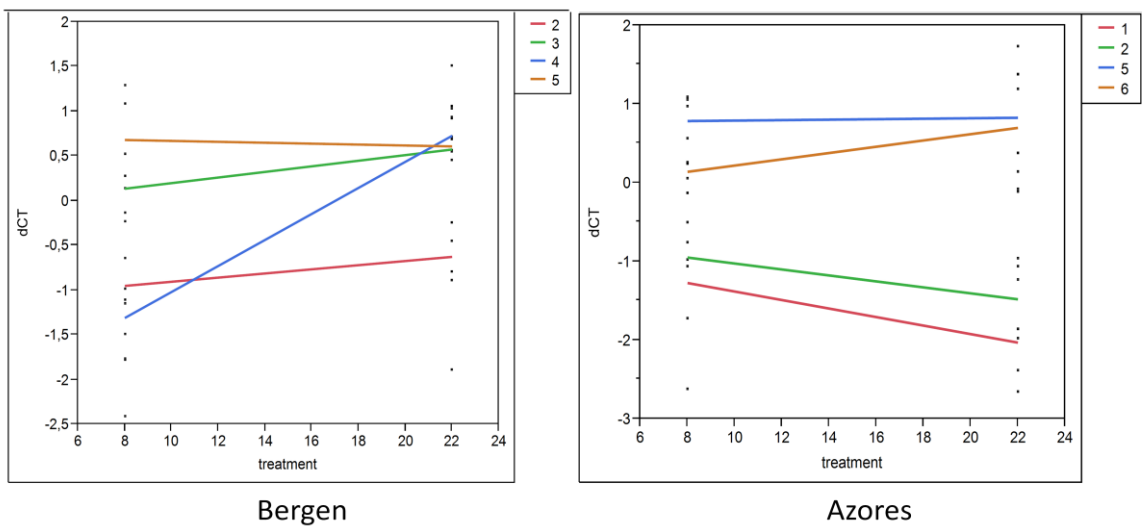


Fig.29: Reaction norms of gene expression. Reaction norms are given for each candidate gene. Left: Bergen, right: Azores. X-axis: Treatment temperature [°C], y-axis: dCT, fold expression change in comparison to the HKG.

Acknowledgments

My special thanks go to Kai Lohbeck for being such an enthusiastic and patient supervisor. I am grateful for all your advice and helpfulness. Thank you for all the effort and time. Further, thanks for all answering all my questions, and for the correction of my thesis. I really learned a lot from you!

I would like to express my sincere acknowledgement to my supervisor Prof. Thorsten Reusch for giving me the opportunity to work in this research group and for answering all my questions. Thanks for reviewing my thesis!

Sincerely thanks go to Prof. Ulf Riebesell for accepting to be my second supervisor and reviewing this thesis.

I especially want to thank my sister Simone for always having “a sympathetic ear for me”. I thank my parents for supporting me and making my studies possible.

I would like to thank Anne Beemelmans for motivating and helping with the gene expression. I also want to thank Katrin Beining and Sören Bolte for advices in the RT-qPCR. I thank Jana Meyer and Lothar Miersch for laboratory assistance during the experiment.

Moreover, I thank my friends Jessica Gier and Ashlie Cipriano for their support.

Finally, thanks to Maximilian Winkel for the realization of my cover.

Declaration of Authorship

I certify that the presented thesis

Local temperature adaptation of the widely distributed coccolithophore *Emiliana huxleyi*

is, to the best of my knowledge and belief, original and the result of my own investigations and that I exclusively used the indicated literature and resources.

I assure that this thesis has not been submitted otherwise in order to obtain academic title.

I agree to include this thesis in the library of the GEOMAR | Helmholtz-Zentrum für Ozeanforschung Kiel and the Christian-Albrechts-Universität, Kiel.

I declare that the master thesis I presented in the written exemplars are identical with that I presented in the electronic version.

Erklärung

Hiermit erkläre ich, die vorliegende Masterarbeit

Local temperature adaptation of the widely distributed coccolithophore *Emiliana huxleyi*

selbstständig und mit keinen anderen als den angegebenen Quellen und Hilfsmitteln angefertigt zu haben.

Ich versichere, dass diese Arbeit nicht an anderer Stelle zur Erlangung eines akademischen Grades vorgelegt wurde.

Mit der Einstellung dieser Arbeit in die Fachbibliothek des GEOMAR | Helmholtz-Zentrum für Ozeanforschung Kiel und in die Universitätsbibliothek der Christian-Albrechts-Universität zu Kiel erkläre ich mich einverstanden.

Ich bestätige, dass die gebundene Arbeit mit der elektronischen Version übereinstimmt.

Kiel, den 23. Oktober 2012

Regina Klapper